Original

Paxian, A.; Sein, D.; Panitz, H.-J.; Warscher, M.; Breil, M.; Engel, T.;
Toedter, J.; Krause, A.; Cabos Narvaez, W.D.; Fink, A.H.; Ahrens, B.;
Kunstmann, H.; Jacob, D.; Paeth, H.:

Bias reduction in decadal predictions of West African monsoon rainfall using regional climate models

Journal of Geophysical Research : Atmospheres (2016) AGU

DOI: 10.1002/2015JD024143

AGU PUBLICATIONS

JGR

Journal of Geophysical Research: Atmospheres

RESEARCH ARTICLE
10.1002/2015JD024143

Key Points:
- RCMs reduce Sahel rainfall bias of GCM predictions but raise Guinea Coast bias
- Coupled atmosphere-ocean RCMs improve both Atlantic SST and WAM rainfall biases
- Improved SST, vegetation, and land cover boundary conditions reduce some biases

Correspondence to:
A. Paxian,
andreas.paxian@uni-wuerzburg.de

Citation:
Paxian, A., et al. (2016), Bias reduction in decadal predictions of West African monsoon rainfall using regional climate models, *J. Geophys. Res. Atmos.*, *121*, 1715–1735, doi:10.1002/2015JD024143.

Received 27 AUG 2015
Accepted 5 FEB 2016
Accepted article online 8 FEB 2016
Published online 29 FEB 2016

Bias reduction in decadal predictions of West African monsoon rainfall using regional climate models

A. Paxian[1], D. Sein[2,3], H.-J. Panitz[4], M. Warscher[5], M. Breil[4], T. Engel[4], J. Tödter[6], A. Krause[5], W. D. Cabos Narvaez[7], A. H. Fink[4], B. Ahrens[6], H. Kunstmann[5], D. Jacob[8], and H. Paeth[1]

[1]Institute of Geography and Geology, University of Würzburg, Würzburg, Germany, [2]Department of Climate Dynamics, Alfred Wegener Institute, Bremerhaven, Germany, [3]P.P. Shirshov Institute of Oceanology, Russian Academy of Science, Saint Petersburg, Russia, [4]Institute of Meteorology and Climate Research—Troposphere Research, Karlsruhe Institute of Technology, Eggenstein-Leopoldshafen, Germany, [5]Institute of Meteorology and Climate Research—Atmospheric Environmental Research, Karlsruhe Institute of Technology, Garmisch-Partenkirchen, Germany, [6]Institute for Atmospheric and Environmental Sciences, Goethe University Frankfurt, Frankfurt/Main, Germany, [7]Department of Physics and Mathematics, University of Alcalá, Madrid, Spain, [8]Climate Service Center, Hamburg, Germany

Abstract The West African monsoon rainfall is essential for regional food production, and decadal predictions are necessary for policy makers and farmers. However, predictions with global climate models reveal precipitation biases. This study addresses the hypotheses that global prediction biases can be reduced by dynamical downscaling with a multimodel ensemble of three regional climate models (RCMs), a RCM coupled to a global ocean model and a RCM applying more realistic soil initialization and boundary conditions, i.e., aerosols, sea surface temperatures (SSTs), vegetation, and land cover. Numerous RCM predictions have been performed with REMO, COSMO-CLM (CCLM), and Weather Research and Forecasting (WRF) in various versions and for different decades. Global predictions reveal typical positive and negative biases over the Guinea Coast and the Sahel, respectively, related to a southward shifted Intertropical Convergence Zone (ITCZ) and a positive tropical Atlantic SST bias. These rainfall biases are reduced by some regional predictions in the Sahel but aggravated by all RCMs over the Guinea Coast, resulting from the inherited SST bias, increased westerlies and evaporation over the tropical Atlantic and shifted African easterly waves. The coupled regional predictions simulate high-resolution atmosphere-ocean interactions strongly improving the SST bias, the ITCZ shift and the Guinea Coast and Central Sahel precipitation biases. Some added values in rainfall bias are found for more realistic SST and land cover boundary conditions over the Guinea Coast and improved vegetation in the Central Sahel. Thus, the ability of RCMs and improved boundary conditions to reduce rainfall biases for climate impact research depends on the considered West African region.

1. Introduction

A rather new climate research field with emerging scientific interest in recent years deals with decadal climate predictions [*Murphy et al*., 2010]. They focus on 10–30 year predictions ranging between seasonal forecasts and climate change projections at the centennial time scale and are particularly required for medium term decision making of planners and policy makers [*Meehl et al*., 2009]. Decadal prediction skill is generated from predictability in both boundary conditions, mainly greenhouse gas (GHG) and aerosol concentrations [*van Oldenborgh et al*., 2012; *Mehta et al*., 2013], and initial conditions, especially the three-dimensional ocean [*Matei et al*., 2012; *Hazeleger et al*., 2013], sea ice, and land surface characteristics [*Bellucci et al*., 2015]. Large influence at the multidecadal time scale has even been reported for atmospheric initial conditions [*Paxian et al*., 2014]. Recent studies have detected some decadal predictive skill in sea surface temperatures (SSTs) of the North Atlantic, Indian, and tropical Pacific Oceans [*Keenlyside et al*., 2008; *Kim et al*., 2012], and first multimodel climate predictions for the forthcoming decade are available [*Smith et al*., 2013].

This study analyzes decadal predictions of the West African monsoon (WAM) rainfall that determines food and water security and economic development in sub-Saharan West Africa [*Benson and Clay*, 1998]. To predict the interannual to decadal WAM rainfall variability the initial and boundary conditions of relevant ocean basins need to be known [*Rodriguez-Fonseca et al*., 2011; *Rowell*, 2013]: The equatorial East Atlantic SSTs reveal strong impacts on the Guinea Coast rainfall but less influence on the Sahel precipitation since the 1970s [*Diatta and*

Fink, 2014] due to counteracting effects of the Atlantic and Pacific Oceans [*Losada et al*., 2012]. Instead, Sahel rainfall is linked to the Atlantic Multidecadal Oscillation and to Indian Ocean and Eastern Mediterranean SSTs [*Diatta and Fink*, 2014]. Multiyear predictability has been found for the tropical Atlantic atmosphere [*Dunstone et al*., 2011]. However, the initialized coupled global general circulation models (GCMs) of the Coupled Model Intercomparison Project phase 5 reveal different decadal predictive skills for Sahel rainfall (measured by anomaly correlation coefficients and root-mean-square errors) due to varying ocean initializations, SST variabilities, and SST rainfall teleconnections [*Gaetani and Mohino*, 2013; *Martin and Thorncroft*, 2014].

The systematic bias of decadal predictions of WAM rainfall is another crucial factor, impeding their use in real decision processes. Even if some biases can be corrected by statistical postprocessing [*Kharin et al*., 2012], the understanding of their causes may improve decadal prediction systems [*Hawkins et al*., 2014]. Indeed, a common problem of many state-of-the-art coupled GCMs over West Africa is overestimated WAM rainfall over the Gulf of Guinea and underestimated Sahel precipitation, reflecting a southward shift of the WAM, and the Intertropical Convergence Zone (ITCZ) [*Martin et al*., 2014; *Richter et al*., 2014]. This displacement of rainfall patterns has been related to positive SST biases in the tropical East and South-East Atlantic Ocean [*Janicot et al*., 1998; *Losada et al*., 2010] which are probably caused by weaker equatorial easterlies in boreal spring deepening the South-East Atlantic thermocline and inhibiting the Benguela cold tongue upwelling [*Richter et al*., 2014]. The reduced easterlies are linked to an ITCZ southward shift [*Tozuka et al*., 2011] or a weaker subtropical anticyclone reducing along-shore winds over South-West Africa and the northward Benguela current [*Richter et al*., 2012]. Further explanations involve fewer stratocumulus clouds [*Hu et al*., 2010] or a coarse horizontal ocean resolution ($>1°$) [*Grodsky et al*., 2012].

To meet the needs of climate impact studies in West Africa high-resolution regional climate models (RCMs) resolving small-scale atmospheric processes and land surface interactions are applied [*Paeth et al*., 2011]. RCM experiments are able to improve the rainfall climatology of global driving data, e.g., over the Mediterranean area [*Paxian et al*., 2015] and Africa [*Sylla et al*., 2010]. The (ENSEMBLES) Ensembles-based Predictions of Climate Changes and Their Impacts multimodel RCM ensemble forced by reanalysis data reveals strongly differing annual rainfall biases between various RCMs in West Africa, often smaller but partly larger than global driving data. The RCM ensemble mean clearly reduces the bias of global reanalyses [*Paeth et al*., 2011]. The recent CORDEX (Coordinated Regional Climate Downscaling Experiment) multimodel RCM ensemble shows similar results for the July, August, and September season [*Nikulin et al*., 2012] and further captures the spatial distribution and annual cycle of the Gulf of Guinea and Sahel rainfall [*Gbobaniyi et al*., 2014]. Improved spatial patterns of West African rainfall have also been found for RCMs forced by AMIP (Atmospheric Model Intercomparison Project)-type GCM data [*Druyan et al*., 2010]. Further added values are provided by high-resolution atmosphere-ocean climate models which are fully coupled at the regional scale and capture fine-scale air-sea interactions, e.g., over the North Atlantic and Europe [*Sein et al*., 2015] and during the Indian summer monsoon [*Ratnam et al*., 2008].

Additional improvements of simulated WAM rainfall bias (and predictability) can be achieved by optimizing the planetary boundary layer, microphysics, or cumulus schemes [*Klein et al*., 2015] and by implementing more realistic nonoceanic initial or boundary conditions which are predictable over a decade in GCMs and RCMs: Besides anthropogenic GHG emissions, the radiative forcing by aerosols, e.g., from mineral dust or biomass burning, impacts on temperature, rainfall, and the large-scale monsoon circulation in West Africa [*Paeth and Feichter*, 2006; *Solmon et al*., 2012]. Large effects on the West African monsoon circulation and rainfall have also been stated for man-made land cover changes like deforestation or desertification via small-scale land-atmosphere interactions [*Abiodun et al*., 2008; *Paeth et al*., 2009]. The use of a land surface parameterization with explicit vegetation representation [*Xue et al*., 2004] and a coupled dynamic vegetation model with fine-scale vegetation-atmosphere feedbacks [*Alo and Wang*, 2010] has improved simulated WAM development and rainfall. Due to their long-term memory, small-scale soil moisture initial and boundary conditions affect WAM rainfall predictability in a hot spot region for land-atmosphere coupling and soil-precipitation feedbacks [*Douville et al*., 2007; *Moufouma-Okia and Rowell*, 2010].

Our study investigates the WAM rainfall biases from global predictions of the new German decadal prediction system [*Pohlmann et al*., 2013] in three West African regions and several hindcast decades. Following recent research work, we address the three main hypotheses that global prediction biases can be improved by dynamical downscaling with (1) a multimodel ensemble of high-resolution RCMs, (2) a RCM coupled to a global ocean model, and (3) a RCM accounting for more realistic boundary conditions like aerosols, SSTs, vegetation,

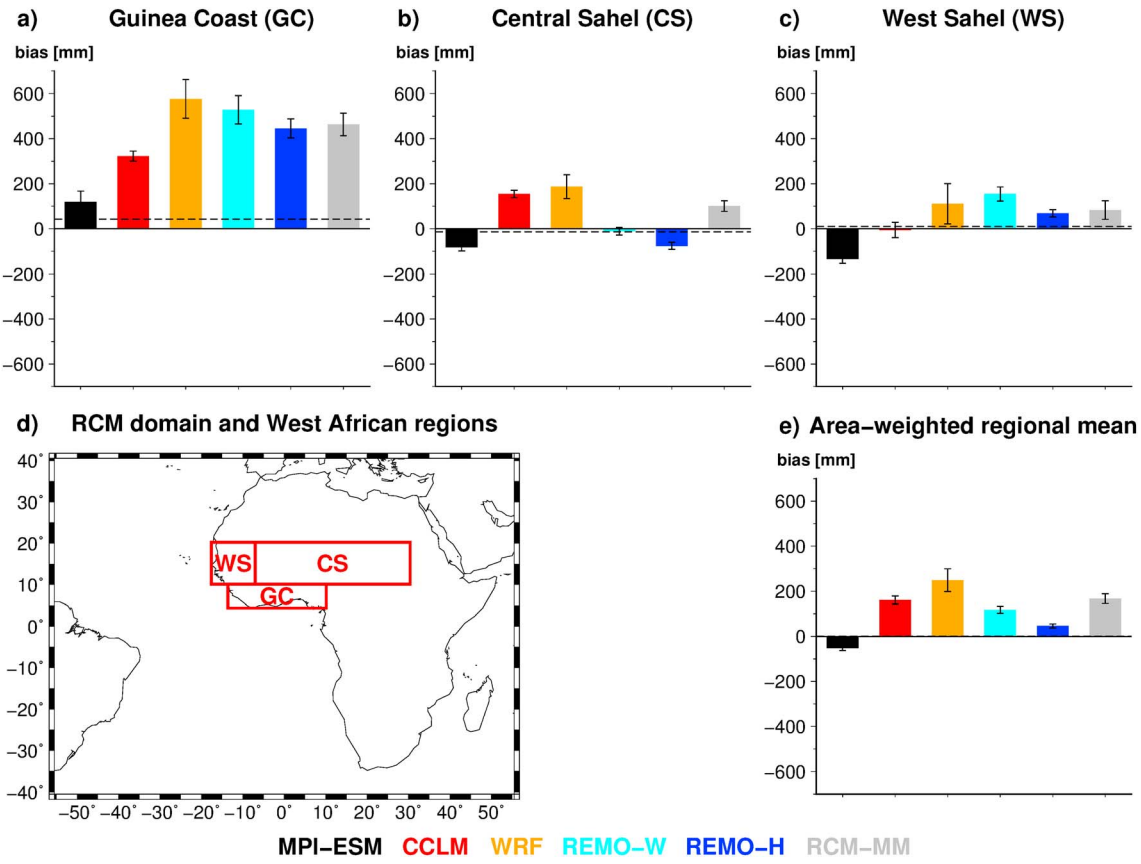

Figure 1. Biases of simulated WAM rainfall from ensemble means of MPI-ESM, different regional predictions and the multimodel RCM ensemble of CCLM, WRF, and REMO-W (RCM-MM) compared to WMMA observations for (a–c) three West African regions and (e) the area-weighted mean of all regions. The bars and error bars describe the means and standard deviations over the JJAS seasons of four hindcast decades, respectively, and the dashed lines mark the corresponding biases of CRU observations compared to WMMA. (d) The schematic map shows the model domain of regional predictions and defines the three West African regions under consideration.

and land cover as well as optimized soil initialization. To test these hypotheses on the beneficial impacts of a high atmospheric resolution, small-scale atmosphere-ocean interactions, and improved atmospheric, oceanic, or terrestrial processes numerous ensembles of regional decadal predictions have been performed with three RCMs in various versions nested into the global predictions. WAM rainfall biases of global and regional predictions are compared with each other, and for prominent bias reductions or increases possible physical process-based explanations are investigated. The following section describes the experimental design of global and regional predictions, the observational data, and the data processing used in this study. The resulting WAM rainfall biases are presented in section 3. Section 4 summarizes and discusses the results and in section 5 the main conclusions are drawn.

2. Data and Methods

In order to investigate WAM rainfall biases in decadal climate predictions initialized coupled GCM experiments have been used and different types of RCM simulations have been performed: (1) a multimodel ensemble of three RCMs nested into the global GCM predictions, (2) two RCM ensembles coupled to the global ocean model of the coupled GCM, and (3) several RCM ensembles accounting for more realistic boundary conditions and improved soil initialization.

2.1. Global Decadal Predictions

The global decadal predictions have been taken from the new version of the Max-Planck Institute for Meteorology Earth System Model Low Resolution (MPI-ESM LR). It is based on the coupled GCM ECHAM6/MPI-OM at T63 (~1.9°) and GR15 (~1.5°) horizontal resolution with 47 and 40 vertical levels in the

Table 1. Number of Available Decadal Prediction Simulations of the Considered GCM and RCM Ensembles, Including Those With Ocean Coupling and Improved Boundary Conditions and Soil Initialization, for Each Considered Hindcast Decade [a]

	Number of Simulations Per Hindcast Decade			
Model (Version)	1966–1975	1981–1990	1991–2000	2001–2010
MPI-ESM	10	10	10	10
WRF	2	2	2	2
REMO-W	3	3	3	3
REMO-H	3	3	3	3
REMO-O1	3	3	3	3
REMO-O2	3	3	3	3
CCLM	3	3	3	3
CCLM-AOD	-	-	-	3
CCLM-AOD/SST	3	-	-	3
CCLM-SOIL	-	-	-	3
CCLM-VEG	-	-	-	3
CCLM-LUC	3	3	3	3
CCLM-LUV	3	3	-	3

[a]For description of models and model versions see data and methods section.

atmospheric and oceanic component, respectively [*Jungclaus et al*., 2013; *Pohlmann et al*., 2013; *Stevens et al*., 2013]. A quasi-realistic MPI-ESM assimilation run has been nudged to ocean temperature and salinity anomalies from the ORAS4 ocean reanalysis [*Balmaseda et al*., 2013] of the European Centre for Medium-Range Weather Forecasts (ECMWF) and to surface pressure, temperature, vorticity, and divergence fields from ERA40 [*Uppala et al*., 2005] and ERA-Interim atmospheric reanalyses [*Dee et al*., 2011] before and after 1990, respectively. From this assimilation run a 10 member ensemble of freely evolving decadal predictions of 10 year length has been initialized in 1 January in every year from 1961 to 2014 with 1 day lagged initialization for each ensemble member, i.e., 10 MPI-ESM members for 54 hindcast decades [*Pohlmann et al*., 2013].

2.2. Regional Decadal Predictions

The dynamical downscaling of the global predictions has been carried out with a multimodel ensemble of three RCMs: (1) the hydrostatic REMO [*Jacob*, 2001; *Jacob et al*., 2007] in version 2009 (REMO-W), (2) the nonhydrostatic COSMO-CLM (CCLM) [*Rockel et al*., 2008] in version 4-21, i.e., the CORDEX-Africa configuration [*Panitz et al*., 2014], and (3) the nonhydrostatic Weather Research and Forecasting (WRF) model [*Skamarock et al*., 2008] in version 3-5-1. In addition, a further REMO version with improved parameterizations for tropical climate simulations, including minimum cloud heights for precipitation formation and soil properties for rainforests, has been applied (REMO-H). These models have been frequently used in studies on the West African climate and found to reproduce the WAM system reasonably well [*Paeth et al*., 2005, 2011; *Flaounas et al*., 2011; *Nikulin et al*., 2012; *Gbobaniyi et al*., 2014; *Kothe et al*., 2014a; *Panitz et al*., 2014].

All RCMs cover the model domain from 59.4°W to 59.4°E and 44°S to 44°N at 0.44° resolution. The 7–8 grid boxes along the lateral boundaries have not been considered for further analyses to avoid artificial boundary effects (cf. Figure 1). To prevent a cold start of the deep soil layers the RCM simulations have been initialized with soil conditions from spin-up simulations forced by ERA40 or ERA-Interim reanalyses depending on the simulated decade. Due to limited computing resources we have decided to downscale three instead of the full 10 MPI-ESM ensemble members for each RCM version during four selected hindcast decades considered as crucial episodes in the historical WAM evolution, i.e., 1966–1975, 1981–1990, 1991–2000, and 2001–2010 (Table 1). The method to select 3 out of 10 MPI-ESM members per decade is as follows: for each decade we have chosen those three global predictions with best, intermediate, and worst skill in correlations to observed SST variations in several oceanic regions most relevant to the WAM rainfall (cf. H. Paeth et al., Decadal and multi-year predictability of the West African monsoon and the role of dynamical downscaling, submitted to *Journal of Climate, 2016*). Due to far higher computing costs, only the best and worst MPI-ESM members per decade have been downscaled with WRF. In all simulations GHG concentrations have been taken from historical observations before 2005 and from the RCP4.5 scenario (Representative Concentration Pathway) [*Moss et al*., 2010] after 2005.

2.3. Coupled Regional Decadal Predictions

Two REMO-H ensembles have been realized for each selected decade which have been fully coupled to the global MPI-OM ocean model component of MPI-ESM within the RCM domain described above [*Sein et al*., 2015]. The two ensembles differ in the assimilation run from which the decadal predictions are initialized: For the REMO-O1 ensemble, the ocean model spin-up has been carried out similarly to the MPI-ESM assimilation run, i.e., MPI-OM has been nudged to ORAS4 ocean reanalyses but forced by ECHAM6 nudged to ERA40/ ERA-Interim atmospheric reanalyses outside the RCM domain and fully coupled with REMO inside this area. For the REMO-O2 ensemble, this spin-up technique has been simplified in directly forcing MPI-OM with ERA40 reanalyses outside the RCM domain instead of using ECHAM6 nudged to atmospheric reanalyses [cf. *Sein et al*., 2014]. The model shock when changing from ERA40 to ECHAM6 forcing in prediction mode has been minimized in keeping the same REMO/MPI-OM setting within the RCM domain as during spin-up.

The MPI-OM configuration differs from that of MPI-ESM and shows a high horizontal resolution within the coupled REMO/MPI-OM domain spanning from 7–25 km near the West African coasts and equatorial Atlantic to 60–65 km at 45°S. It comprises 40 vertical levels. Outside the RCM domain MPI-OM has been driven by atmospheric forcing and reaches a maximum grid-box spacing of 130 km near South Australia [cf. *Sein et al*., 2015, Figure 27d]. The interactions between global ocean with regionally high resolution and regional atmosphere are expected to strongly improve the simulation of regional climate due to better resolved land-sea contrasts and air-sea exchanges of energy, mass, and momentum [*Sein et al*., 2015].

2.4. Regional Decadal Predictions With Improved Boundary and Initial Conditions

Several CCLM ensembles with more realistic aerosol, SST, vegetation, and land cover boundary conditions as well as improved soil initialization have been performed:

1. The standard CCLM aerosol optical depth (AOD) climatology from *Tanré et al*. [1984] which is constant in time at a very low resolution of T10 (~11.25°) has been exchanged by the improved AOD climatology from the AeroCom project [*Kinne et al*., 2006] offering monthly data for year 2000 conditions at 1° resolution (CCLM-AOD).
2. Additionally, the simulated SSTs from the global MPI-ESM predictions have been replaced by the more realistic SSTs from ERA40 or ERA-Interim reanalyses depending on the simulated decade (CCLM-AOD/SST) in order to reduce simulated SST biases. The CCLM-AOD ensemble has been realized for the 2001–2010 decade and the CCLM-AOD/SST ensemble for 1966–1975 and 2001–2010.
3. The CCLM-SOIL ensemble for the 2001–2010 decade has been initialized by optimized soil temperature and moisture fields from an offline spin-up simulation of CCLM's land surface module TERRA_ML [*Schrodin and Heise*, 2002] during 1979–2000 forced by realistic atmospheric data from WATCH-WFDEI [*Weedon et al*., 2014], a similar approach to the recent ECMWF land reanalysis [*Balsamo et al*., 2015].
4. The CCLM-VEG ensemble has been performed in 2001–2010. It has been coupled to the more sophisticated soil-vegetation-atmosphere-transfer (SVAT) module VEG3D [*Braun and Schädler*, 2005] with explicit vegetation layer replacing CCLM's standard SVAT TERRA_ML in order to improve the simulated interactions between soil, vegetation, and atmosphere [*Breil*, 2015].
5. The CCLM-LUC and CCLM-LUV ensembles have been forced by constant and yearly varying GLC2000 land use maps [*Bartholomé and Belward*, 2005], respectively, substituting the standard constant ECOCLIMAP data [*Champeaux et al*., 2005] during all four hindcast decades except for CCLM-LUV in 1991–2000. The yearly land use changes have been generated by the advanced stochastic land use change model (ASLUCM) (T. Engel, manuscript in preparation, 2015) applying statistics on population, agriculture, desertification, and deforestation from the Food and Agriculture Organization (FAO) (unpublished data, 2015, available from the FAO website, faostat3.fao.org) and street data from the OpenStreetMap contributors (unpublished data, 2015, available from OpenStreetMap, www.openstreetmap.org).

2.5. Observational Data

For the validation of simulated WAM rainfall and SSTs and the assessment of biases in global and regional predictions, different global gridded observational data sets have been applied covering mostly all considered hindcast decades. High-resolution long-term station-based terrestrial precipitation data have been derived from C. J. Willmott and K. Matsuura (WMMA) (unpublished data, 2001, available from the University of Delaware, http://climate.geog.udel.edu/~climate/html_pages/Global2011/Precip_revised_3.02/README.GlobalTsP2011.

html) at 0.5° resolution during 1900–2010 for the analysis of land-only precipitation. Combined satellite and gage data from the Global Precipitation Climatology Project (GPCP) at 2.5° since 1979 [*Adler et al.*, 2003; *Huffman et al.*, 2009] and at 1° since 1996 [*Huffman et al.*, 2001] have been used for the analysis of precipitation over land and ocean as well as the ITCZ position. For SST validation, high-quality data of the operational ocean reanalysis system ORAS4 of the ECMWF at 1° resolution during 1958–present have been applied [*Balmaseda et al.*, 2013].

2.6. Data Processing

The yearly WAM rainfall has been defined as accumulated precipitation during the June to September season (JJAS). Land-only regional means have been analyzed for three regions of homogeneous rainfall variability in sub-Saharan West Africa following *Nicholson and Palao* [1993]: the West Sahel (17.60°W–7.04°W, 10.12°N–20.24°N), Central Sahel (7.04°W–30.36°E, 10.12°N–20.24°N), and Guinea Coast (13.64°W–10.12°E, 4.40°N–10.12°N, cf. Figure 1). The intensity of the WAM rainfall in different regions strongly depends on the latitudinal position of the ITCZ. *Ramage* [1995] have described various ITCZ definitions based on the surface trough, wind convergence, or maximum cloudiness clearly diverging over West Africa. Being aware of this problem, this study follows its identification as maximum rainy zone [*Fink et al.*, 2010], i.e., the maximum of the zonal mean monthly precipitation over all land and ocean grid boxes from 10°W to 10°E averaged over the JJAS season of each year. Sahel rainfall is further linked to the position and strength of the midtropospheric African easterly jet (AEJ) and the associated African easterly waves (AEWs). The AEJ axis is determined by the zero contour line of the shear vorticity of the smoothed 700 hPa wind field that is located in a wind maxima region [*Berry et al.*, 2007], and the AEW activity is defined by the 2–6 days bandpass filtered variance of the 700 hPa meridional wind [cf. *Fink and Reiner*, 2003], again averaged over the JJAS season per year. Accordingly, means of SSTs and other considered variables have been calculated for the JJAS period.

The biases of decadal predictions in regional mean WAM rainfall, ITCZ position, and SSTs are defined as the differences between three-member ensemble means of MPI-ESM, different RCMs, or RCM versions and observations averaged over all years of a certain decade. This study focuses on the model bias of rainfall totals neglecting extreme values because the latter may be controlled by clearly different physical processes than totals which has already been supposed for the Mediterranean area [*Paxian et al.*, 2015]. However, similar analyses of WAM rainfall extremes are planned for future studies. The multiyear and decadal predictability of the prevailing multimodel RCM ensemble for WAM rainfall has been investigated in a parallel study (H. Paeth and 14 coauthors, manuscript in preparation, 2015).

3. Results

In this section the WAM rainfall biases of the global and the different regional decadal predictions are compared with each other. In addition, the results of the coupled regional predictions are shown. Finally, the biases of the regional predictions applying improved boundary conditions and soil initialization are described.

3.1. Global and Regional Decadal Predictions

For the three West African regions, Figure 1 shows the WAM rainfall biases of global and regional predictions compared to land-only WMMA observations which are available for the four selected decades. The biases are averaged over all hindcast decades, and the small error bars denote rather minor variations across different decades, contrary to *Reifen and Toumi* [2009] which do not find such a quite consistent model performance over time. WRF reveals a slightly larger interdecadal standard deviation due to its smaller ensemble size of two members per decade. The observational uncertainty is represented by the corresponding biases of gridded Climatic Research Unit (CRU) observations [*Mitchell and Jones*, 2005, updated] compared to WMMA which are rather small in the Guinea Coast region (43 mm, 5% of WMMA mean) and negligible in the Sahel (10–14 mm, 2–4%).

On average, the global MPI-ESM predictions overestimate WMMA by 120 mm (13%) in the Guinea Coast region and underestimate observations by 83 mm (26%) in the Central Sahel and 135 mm (26%) in the West Sahel. These GCM biases can be clearly reduced by dynamical downscaling with REMO-W (11 mm, 3%) in the Central Sahel and with CCLM (6 mm, 1%) in the West Sahel. The latter is improved by WRF on average as well, but a large interdecadal spread prevails. For other RCMs slightly larger biases are found. This is exceptionally true for the Guinea Coast region where all RCMs strongly aggravate the positive MPI-ESM bias, especially WRF and REMO-W reach average biases of 529–577 mm (59–65%). Overall, the multimodel ensemble mean

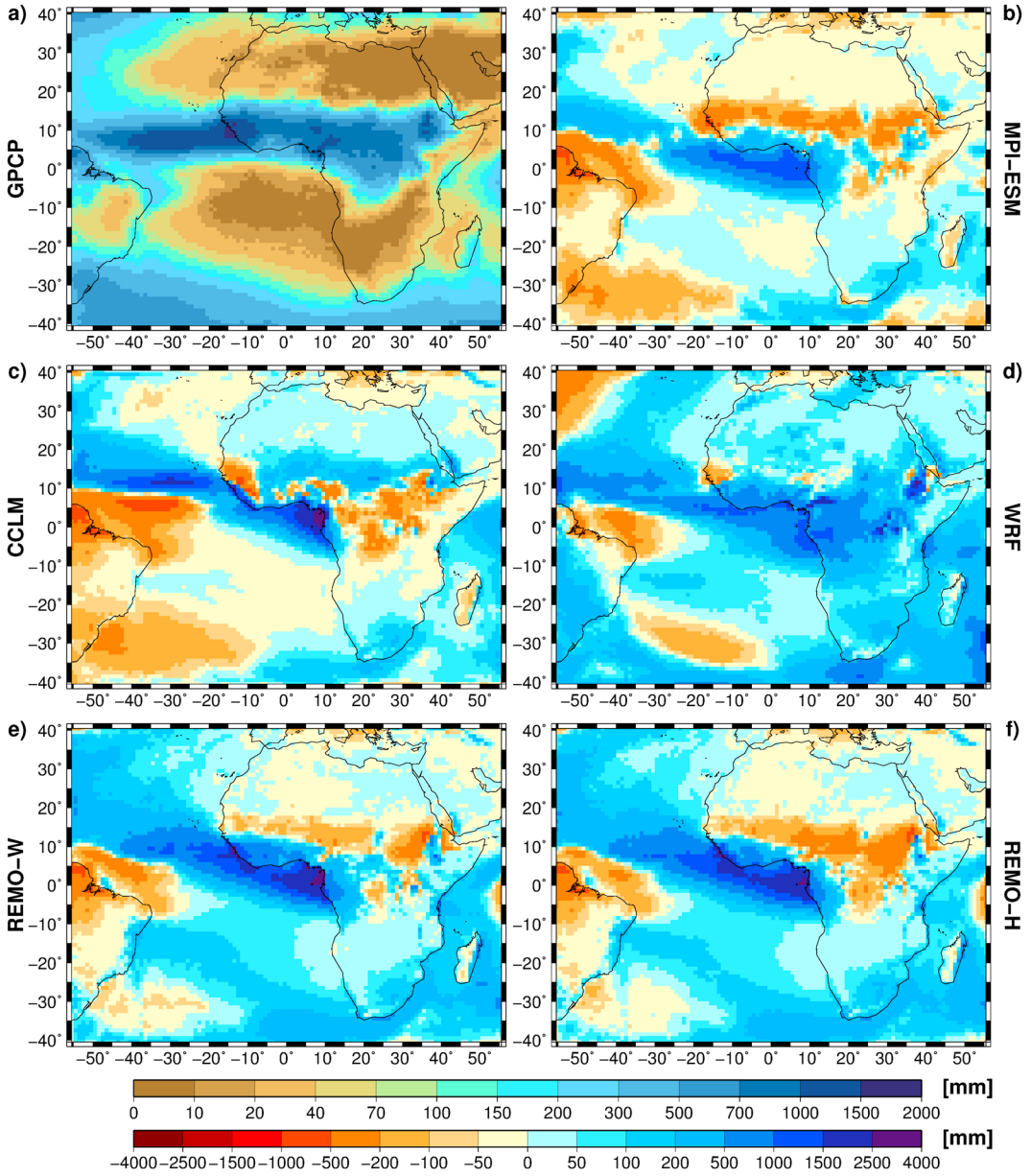

Figure 2. Observed WAM rainfall totals from (a) GPCP at 1° horizontal resolution during the JJAS season of the 2001–2010 decade and corresponding biases of simulated WAM rainfall from (b) ensemble means of MPI-ESM and (c–f) different regional predictions (interpolated to the 1° GPCP grid).

of the CCLM, WRF, and REMO-W standard versions reveals larger biases than the GCM in the Guinea Coast (464 mm, 52%) and Central Sahel regions (100 mm, 32%) but a clear improvement in the West Sahel (83 mm, 16%) with some interdecadal spread. The improved parameterizations of REMO-H are able to slightly reduce the biases of the standard version REMO-W in the Guinea Coast and West Sahel regions, even reducing the MPI-ESM bias to 69 mm (13%) in the latter, but lead to some more underestimation in the Central Sahel. These drier conditions are mainly caused by increased minimum cloud heights for rainfall formation. Further sensitivity studies with WRF show improved biases in both Sahel regions due to optimized model configurations in terms of cumulus parameterization as well as planetary boundary layer and microphysics schemes (not shown). Finally, the area-weighted mean bias of the three regions is analyzed representing an overall larger-scale assessment over the whole West Africa. A small negative MPI-ESM bias (53 mm, 12%) faces larger positive biases of all standard RCMs and their multimodel ensemble mean but is slightly reduced by REMO-H with improved parameterizations (46 mm, 10%).

Thus, the first hypothesis that dynamical downscaling is able to reduce the WAM rainfall biases of global decadal predictions can be partly confirmed for different RCMs in the West (CCLM, REMO-H) and Central Sahel (REMO-W) but must be clearly rejected for all RCMs in the Guinea Coast region. For the whole West Africa, only REMO-H is able to slightly reduce the rather small MPI-ESM bias. The multimodel ensemble mean can improve the GCM in the West Sahel. However, it cannot outperform the results of all RCMs but is defeated by at least one of them in every region and is therefore not considered in the following analyses.

In order to understand the WAM rainfall biases of different global and regional predictions and West African regions, especially the Guinea Coast, a closer look is taken at the observed and simulated spatial precipitation patterns within the considered RCM domain (Figure 2). For the analysis of WAM rainfall over land and ocean GPCP observations are applied during all decades except for 1966–1975. Due to improved data availability, especially of satellite observations, the following analyses are shown for the 2001–2010 decade. However, similar results are found as well for other decades (not shown). The GPCP observations show the typical spatial WAM rainfall pattern: the ITCZ lies over the tropical Atlantic and West Africa at around 8–10°N and yields precipitation maxima of 1700 mm and 1300 mm near the western Guinean and Cameroon mountains, respectively, separated by the drier Dahomey Gap [*Chatelain et al*., 1996]. The global MPI-ESM predictions overestimate observations by up to 1300 mm over the Gulf of Guinea and 500 mm over the Guinea Coast and underestimate GPCP by up to 400 mm over the West and Central Sahel, probably indicating a southward shift of the simulated ITCZ. The RCMs produce even larger positive biases over the Gulf of Guinea, the tropical Atlantic, and the Guinea Coast reaching maxima of 3000–3500 mm for CCLM and REMO-W and 2000 mm for WRF over the eastern Gulf of Guinea. In the Sahel less underestimations than MPI-ESM and even overestimations of observations (for CCLM and WRF) can be found. Thus, the ITCZ seems to be shifted southward and increased in intensity. Again, REMO-H produces drier conditions than REMO-W, especially over land, which becomes apparent in smaller overestimations along the Guinea Coast and larger underestimations in the Sahel. Thus, dynamical downscaling is not able to clearly improve the overall MPI-ESM bias over the whole West Africa, but regional bias reduction is found dependent on the considered region and model and consistent over all decades, e.g., in the Sahel (cf. Figure 1). Consequently, two questions can be raised: What causes the WAM rainfall biases in global decadal predictions and why are they intensified over the Guinea Coast and partly reduced over the Sahel in regional predictions?

In order to find some possible physical explanations for the second question on the reasons for the stated increases and reductions of GCM rainfall biases in RCMs an exemplary comparison of different atmospheric variables impacting the WAM rainfall between global MPI-ESM and regional REMO-W and CCLM predictions is done, again for the 2001–2010 decade (Figure 3): Over the tropical North Atlantic positive and negative MPI-ESM rainfall biases northeast and southwest of the region 8–10°N/55–30°W, respectively, denote a northeastward shift of the ITCZ defined as maximum rainy zone (cf. Figure 2) probably linked to higher spring rainfall over the Gulf of Guinea [*Siongco et al*., 2015]. Larger RCM biases describe a stronger ITCZ shift which might be related to differing convection parameterization schemes influencing the ITCZ position despite identical SST forcing [*Möbis and Stevens*, 2012] and trigger a stronger northward shift of the Hadley cell including the Azores high. Smaller land-sea thermal contrasts due to lower Sahel temperatures in RCMs (not shown) might further weaken the Azores high [*Miyasaka and Nakamura*, 2005]. Thus, Figure 3 reveals decreased sea level pressures south of the latter in both RCMs compared to MPI-ESM, further west for REMO than for CCLM probably due to a more western AEJ position (see below), causing stronger westerlies over the tropical North Atlantic similar to the West African westerly jet [*Pu and Cook*, 2010]. The evaporation and latent heat fluxes over this area and the Gulf of Guinea are intensified compared to MPI-ESM despite the same SST forcing due to increased advection of warm Caribbean air masses by stronger westerlies, especially for REMO-W with more direct westerly flow, and probably differing parameterizations of small-scale turbulent air-sea exchange fluxes. Thus, higher liquid water content is generated and transported by the stronger westerlies toward the Guinea Coast producing increased rainfall amounts, larger for REMO-W than for CCLM due to the higher evaporation. In addition, CCLM reveals stronger southerlies over the Gulf of Guinea related to higher pressures over the South Atlantic and generating more Guinea Coast rainfall and less over the Congo Basin.

Concerning Sahel rainfall biases, the activity of the AEJ and AEWs is analyzed over a slightly smaller area than the RCM domain [*Fink and Reiner*, 2003], but only AEWs are shown in Figure 3 due to rather similar results. Yet differences are found between RCMs probably due to various impacts of land surface conditions: CCLM reveals increased and decreased latent heat fluxes over the Sahel and the Guinea Coast as well as increased and decreased temperatures over Egypt and the Sahel, respectively (not shown), causing a northward shift of

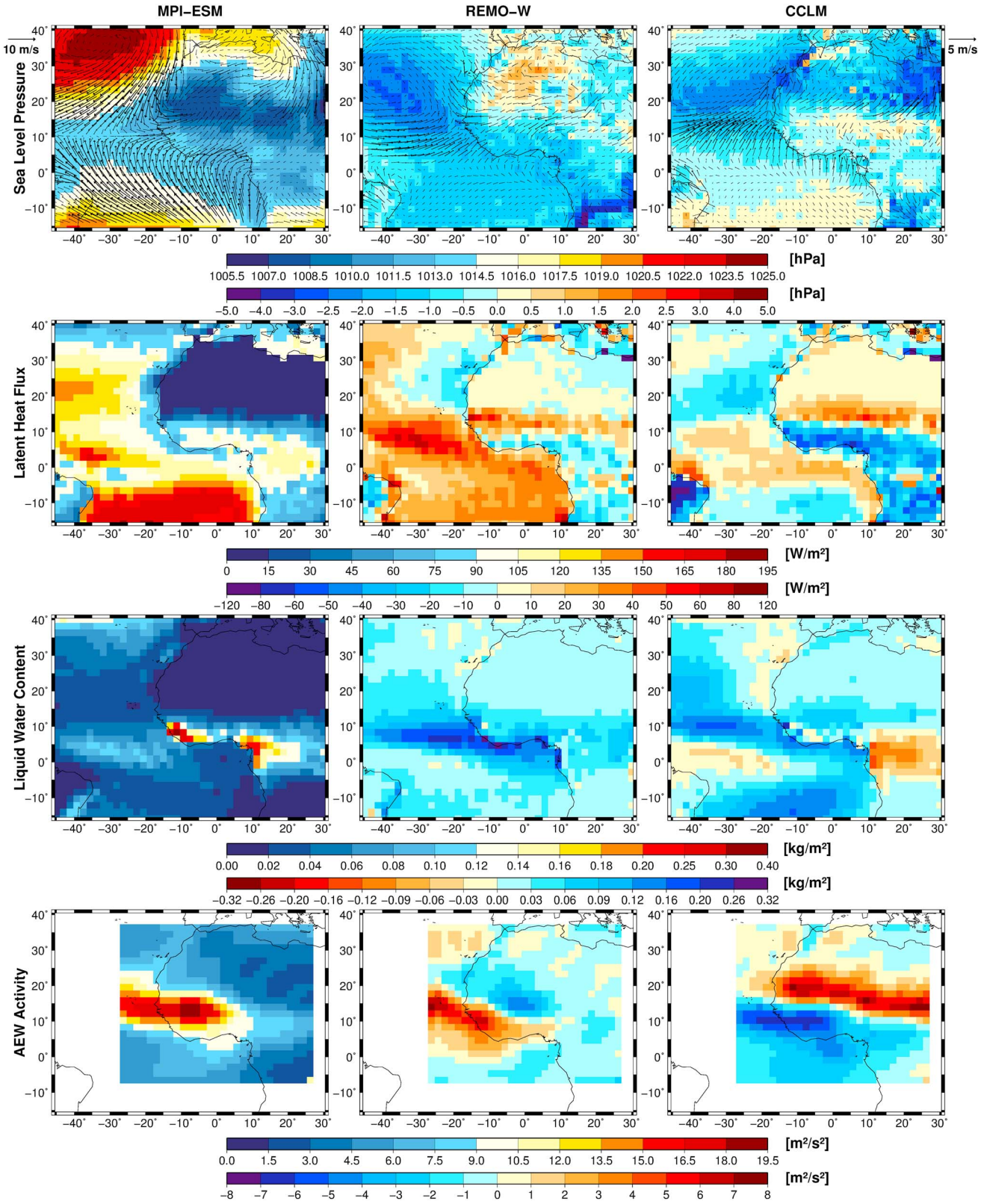

Figure 3. Different atmospheric variables influencing the simulated WAM rainfall from (left) ensemble means of MPI-ESM at T63 horizontal resolution (~1.9°) averaged over the JJAS season of the 2001–2010 decade and (middle) corresponding differences and difference vectors (RCM – GCM) from REMO-W and (right) CCLM regional predictions (interpolated to the T63 MPI-ESM grid): sea level pressure (map) with 10 m wind vectors (arrows) (first row), latent heat flux (second row), liquid water content (third row), and African Easterly Wave activity (fourth row).

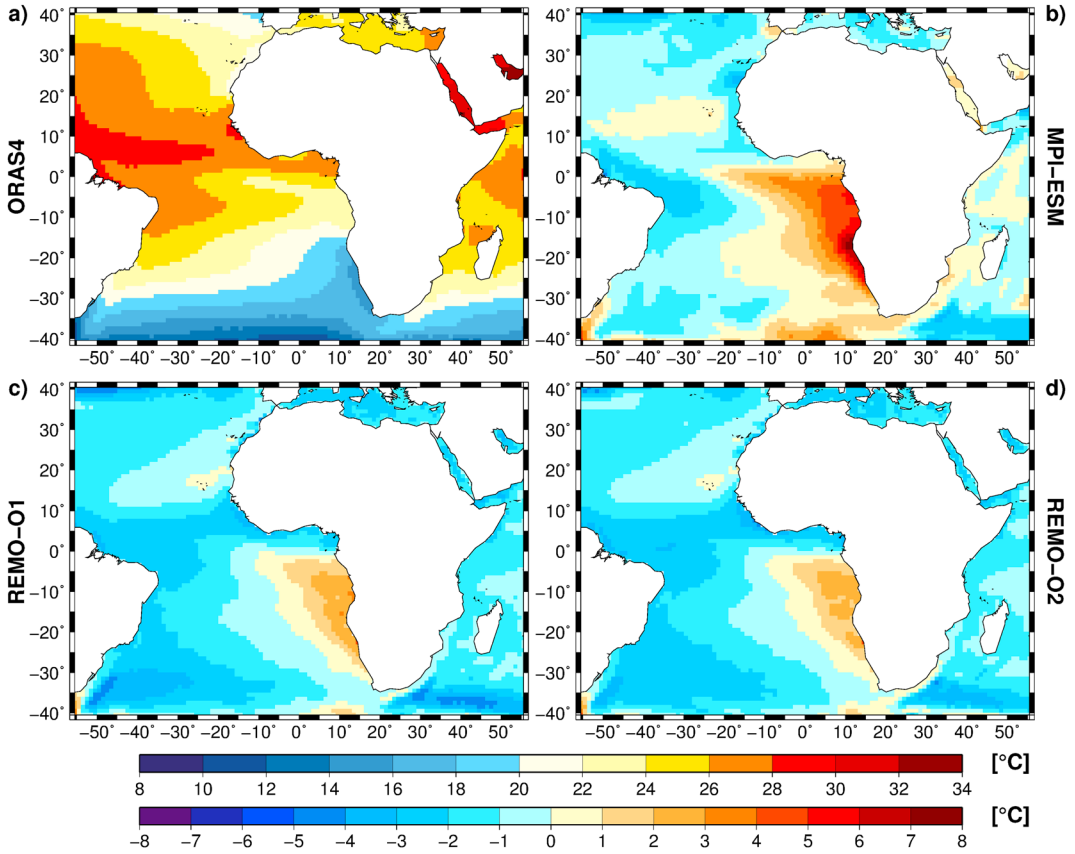

Figure 4. (a) Observed SST means from ORAS4 at 1° horizontal resolution during the JJAS season of the 2001–2010 decade and (b) corresponding biases of simulated SSTs from ensemble means of MPI-ESM and (c–d) different regional predictions coupled to the MPI-OM ocean model (interpolated to the 1° ORAS4 grid).

temperature and moisture gradients and thus of the AEJ and AEWs compared to MPI-ESM [cf. *Cook*, 1999]. REMO-W shows similar but weaker patterns and increased latent heat fluxes in the West Sahel slightly intensifying the AEJ and AEWs and inducing a westward shift. Thus, CCLM clearly overestimates Central Sahel rainfall due to the AEW northward shift, and REMO-W reveals larger rainfall than MPI-ESM probably because a slightly smaller AEW activity is compensated by slightly larger liquid water contents. REMO-W overestimates West Sahel rainfall because of westward shifted AEWs and stronger Atlantic westerlies. The AEW northward shift in CCLM is balanced in this region, but increased westerlies produce more rainfall than MPI-ESM. Intensified AEW activity might even impact Guinea Coast rainfall in REMO-W. Thus, some physical explanations for stated rainfall bias increases or reductions of RCMs can be identified, but clear attributions to single physical processes are often rather difficult because rainfall is generated by a chain of various processes and affected by numerous interactions between them.

Furthermore, we aim to find some possible physical explanation for the first question about the general causes of the WAM rainfall biases in global decadal predictions which are supposed to be related to a possible southward displacement of the simulated ITCZ. Such southward shifts of both monsoon and ITCZ over West Africa have been linked to positive SST biases over the tropical East and South-East Atlantic [*Janicot et al.*, 1998; *Losada et al.*, 2010]. Therefore, Figure 4 provides an insight into observed and simulated SST patterns within the selected RCM domain during the 2001–2010 decade. The ORAS4 reanalyses show the typical zonal SST distribution around Africa superimposed by cold and warm ocean currents propagating toward the equator and the poles near the west and east continental coasts, respectively, with maxima of 29–32°C in the tropical Atlantic and Red Sea and minima of 14–16°C in the South-East Atlantic. In fact, the global MPI-ESM predictions reveal a strong positive SST bias of up to 5–7°C following the course of the Benguela ocean current in the tropical East and South-East Atlantic which probably reduces the sea level pressure gradient

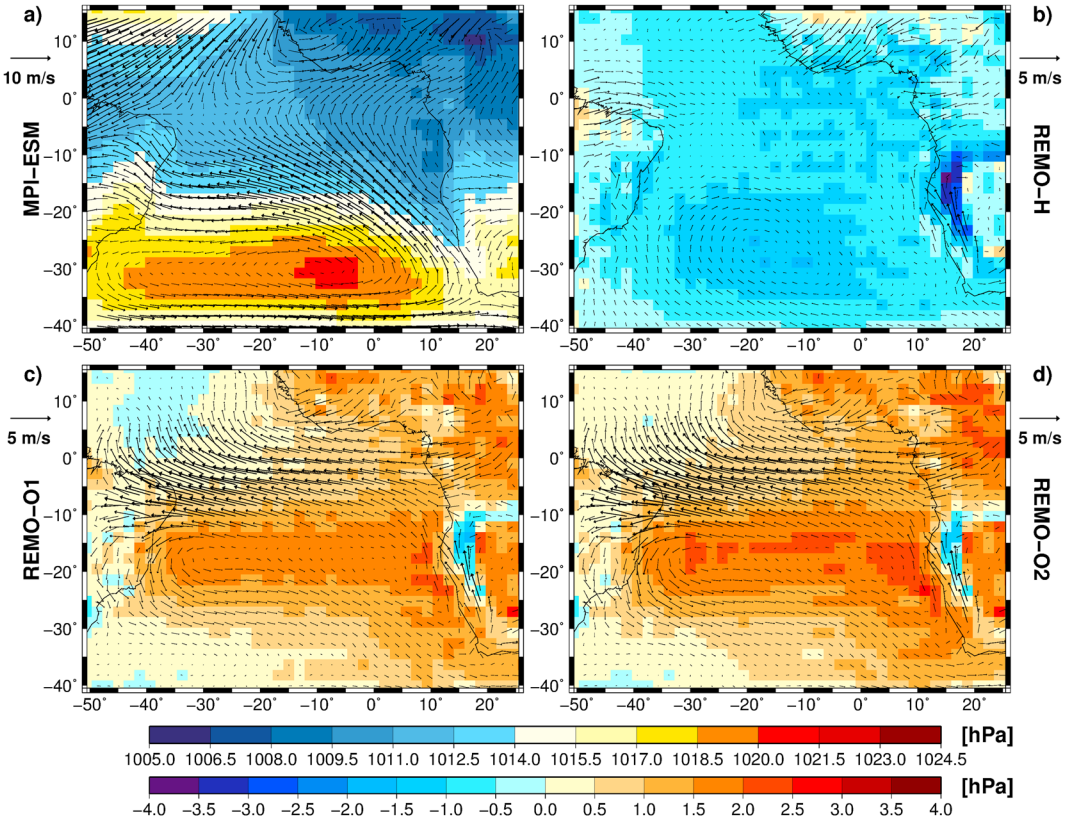

Figure 5. Simulated sea level pressure (map) and 925 hPa wind vector (arrows) means from (a) ensemble means of MPI-ESM at T63 horizontal resolution (~1.9°) averaged over the MAM season of the 2001–2010 decade and (b) corresponding differences and difference vectors (RCM – GCM) from different regional predictions in standard version and (c–d) coupled to the MPI-OM ocean model (interpolated to the T63 MPI-ESM grid).

between Saharan heat low and equator (cf. Figure 3), diminishes the WAM circulation and displaces it farther south [*Losada et al.*, 2010]. Yet this possible driver of the described WAM rainfall biases in MPI-ESM might be superimposed by further impact factors, e.g., land surface conditions or large-scale circulation, and the stated African rainfall biases and the shifted ITCZ may feed back onto the Atlantic SST bias in this coupled atmosphere-ocean GCM [*Tozuka et al.*, 2011; *Richter et al.*, 2012] impeding to disentangle cause and effect. The positive SST bias of MPI-ESM is passed on to all uncoupled RCMs which modify the corresponding WAM rainfall biases due to altered regional-scale processes in the Guinea Coast and Sahel regions as described before (cf. Figure 3).

3.2. Coupled Regional Decadal Predictions

In order to improve the tropical East and South-East Atlantic SST and, hence, the WAM rainfall biases of the global predictions, regional predictions with REMO-H fully coupled to the global MPI-OM ocean model within the selected RCM domain have been performed. Figure 4 (bottom) reveals that the Atlantic SST biases of coupled regional predictions are strongly reduced to 2–3°C maximally. The coupled version REMO-O2 with simplified spin-up procedure reaches similar or even slightly larger improvements than the REMO-O1 version with more sophisticated spin-up.

A possible physical explanation for this improved SST bias is found when comparing simulated sea level pressures and 925 hPa wind vectors during the MAM (March, April, and May) season of the 2001–2010 decade from global, uncoupled, and coupled regional predictions (Figure 5): MPI-ESM successfully simulates the South Atlantic high-pressure system and corresponding south-east trade winds. However, weak southerlies along the South-West African coast inhibit local upwelling of cold water, and equatorial westerlies accompanied by eastward surface ocean currents (opposed to observations) carry warm water toward the Gulf of

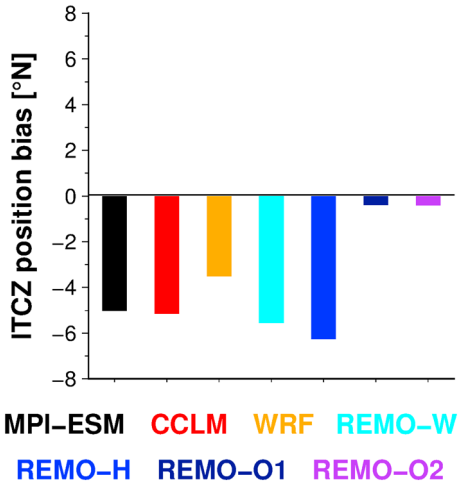

Figure 6. Biases of simulated latitudinal ITCZ position from ensemble means of MPI-ESM and different regional predictions in standard version and coupled to the MPI-OM ocean model compared to GPCP observations during the JJAS season of the 2001–2010 decade.

Guinea and further southward [cf. *Grodsky et al.*, 2012; *Richter et al.*, 2012, 2014]. The uncoupled REMO-H regional prediction increases along-shore southerlies over Namibia and easterlies over West and Central Africa probably due to improved representation of regional topography but changes over the ocean are suppressed by the driving MPI-OM oceanic boundary condition which is prescribed every 6 h. The coupled regional predictions reveal similar wind patterns over land, a South Atlantic high-pressure system of larger magnitude expanding further northward (shifting as well the near-equatorial wind convergence zone) and strongly intensified easterlies and westward surface ocean currents over the whole tropical Atlantic. These changes appear slightly stronger in REMO-O2 than in REMO-O1. Thus, the combination of high atmosphere and ocean model resolutions and their interaction via fine-scale air-sea exchanges enhance the cold water upwelling of the Benguela current and limit the southward expansion of the warm Angola current, altogether reducing the Atlantic SST bias [cf. *Grodsky et al.*, 2012].

Furthermore, the bias of the latitudinal ITCZ position over West Africa from global and regional predictions compared to GPCP observations during the 2001–2010 decade is shown (Figure 6). The aim is to analyze the assumption of a systematic ITCZ southward shift in the GCM and all uncoupled RCMs and to assess possible improvements in the coupled RCM. In fact, MPI-ESM reveals a clear ITCZ position bias of −5°N denoting a strong southward shift of the observed position at 9.5°N over the northern Guinea Coast region to 4.5°N over the northern Gulf of Guinea which agrees well with the WAM rainfall bias pattern. The regional predictions show slightly stronger southward shifts of up to −6°N (REMO-H) except for WRF which reduces the MPI-ESM bias to −3.5°N because its rainfall bias maxima over the Gulf of Guinea are located further north than those of all other models (see Figure 2). Thus, the stated rainfall bias reductions and increases of RCMs compared to MPI-ESM may arise from the interaction of different processes: the ITCZ southward shift related to the inherited SST bias from MPI-ESM and the rainfall bias modifications due to altered regional-scale mechanisms as shown for REMO-W and CCLM (see Figure 3). Both versions of coupled regional predictions are able to

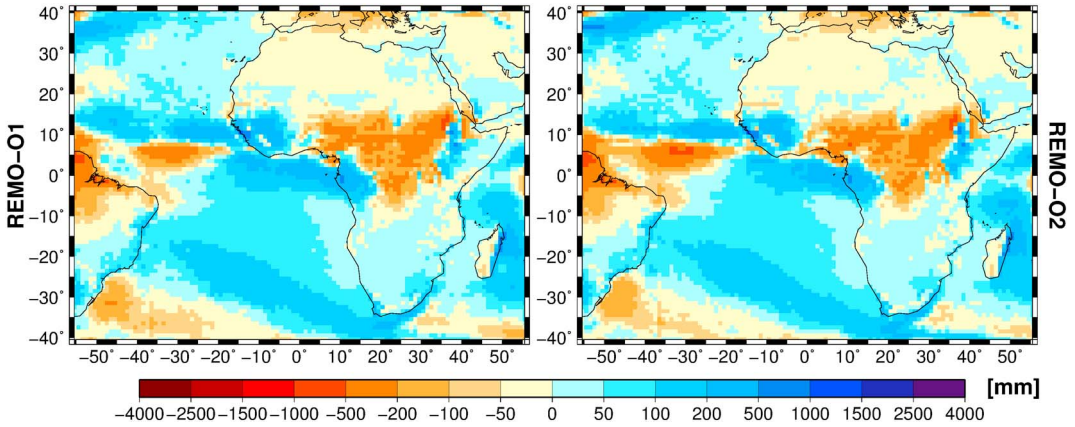

Figure 7. Biases of simulated WAM rainfall from ensemble means of different regional predictions coupled to the MPI-OM ocean model compared to GPCP observations (interpolated to the 1° GPCP grid) during the JJAS season of the 2001–2010 decade.

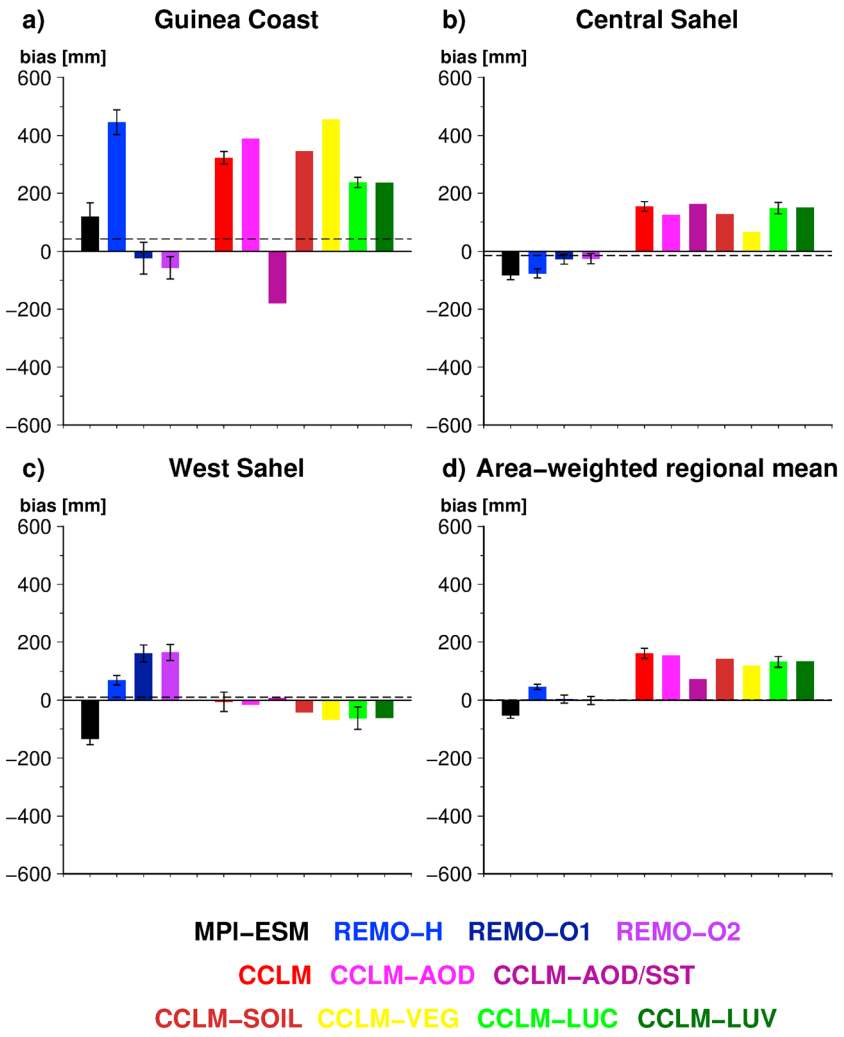

Figure 8. Biases of simulated WAM rainfall from ensemble means of MPI-ESM and different regional predictions in standard version, coupled to the MPI-OM ocean model and applying improved boundary conditions (aerosols, SSTs, vegetation, and land cover) and soil initialization compared to (a–c) WMMA observations for three West African regions and (d) the area-weighted mean of all regions. The bars describe the means over the JJAS seasons of all available hindcast decades (cf. Table 1), and the error bars show the corresponding standard deviations only if all four decades are available. The dashed lines mark the corresponding biases of CRU observations compared to WMMA.

reduce the ITCZ position bias to almost zero and successfully reproduce the observed position over the northern Guinea Coast probably due to the strongly improved Atlantic SST bias.

Subsequently, the simulated spatial patterns of WAM rainfall biases from coupled regional predictions compared to GPCP observations are analyzed during the 2001–2010 decade (Figure 7). Both coupled versions reveal rather similar results: strongly reduced positive biases of up to 400 mm (or even negative biases) over the tropical Atlantic, the Gulf of Guinea, and the Guinea Coast and less intensive negative biases in both Sahel regions compared to uncoupled REMO-H and MPI-ESM predictions. However, more widespread positive biases of up to 400 mm can be found in the West Sahel. The strong north-south gradient in WAM rainfall biases of REMO-H and MPI-ESM predictions is replaced by a slight east-west gradient, reflecting no latitudinal ITCZ shift. Similar results to all previous analyses presented for the 2001–2010 decade can be stated as well for other decades (not shown).

Figure 8 presents the final look at the three considered West African regions over all available hindcast decades similar to Figure 1 and confirms that both versions of coupled regional predictions strongly reduce the large WAM rainfall biases of REMO-H and MPI-ESM in the Guinea Coast region to 23–57 mm (3–6%). Slight

improvements can further be stated in the Central Sahel (25–27 mm, 8–9%) but not in the West Sahel (161–164 mm, 31%). REMO-O1 performs slightly better than REMO-O2 in the Guinea Coast region. Overall, the area-weighted regional mean for the whole West Africa reveals a clear reduction of the already small MPI-ESM bias to almost zero (1–3 mm, 0–1%). The small error bars denote rather little variations between different decades and show a slightly larger variability only for the Guinea Coast where higher rainfall sums prevail. Thus, the second hypothesis that regional decadal predictions coupled to a global ocean model are able to improve WAM rainfall biases can be clearly verified in the Guinea Coast and Central Sahel regions and even for the whole West Africa.

3.3. Regional Decadal Predictions With Improved Boundary and Initial Conditions

Finally, the WAM rainfall biases of the RCM predictions with improved boundary conditions and soil initialization compared to WMMA observations are investigated for the three West African regions (Figure 8). In contrast to Figure 1, the biases are averaged over all available hindcast decades (cf. Table 1), and the error bars are only given if four decades are existent. CCLM-LUC reveals small error bars signifying rather minor variations across all four decades with slightly larger deviations in the West Sahel. Similarly low variability between the available two and three decades is found as well for CCLM-AOD/SST and CCLM-LUV, respectively (not shown).

The improved AOD climatology of CCLM-AOD slightly reduces the CCLM bias in the Central Sahel but deteriorates the result in the Guinea Coast region. The more realistic ERA-Interim SSTs (CCLM-AOD/SST) strongly diminish the SST bias of global predictions (not shown) and the CCLM rainfall bias in the Guinea Coast region (similar to coupled regional predictions) but cause an underestimation of observed precipitation (179 mm, 20%). In the West Sahel dynamical downscaling with combined AOD and SST improvements reduces the global prediction bias to almost zero (8 mm, 2%), though not further improving the CCLM result. However, the use of SSTs from reanalysis data is restricted to present-day conditions. Therefore, sensitivity studies with statistical bias correction have been performed which apply decadal-mean monthly correction factors between MPI-ESM and ERA-Interim SSTs to simulated values, preserve the simulated variability, and allow the application to future predictions without reanalysis data. The corresponding results are similar to those of the CCLM-AOD/SST ensemble and therefore not shown.

The improved soil initialization of CCLM-SOIL reveals a slightly reduced WAM bias in the Central Sahel but slightly larger ones in the other regions. Another sensitivity study of CCLM-SOIL has been performed in which additionally satellite-based Climate Change Initiative (CCI) retrievals of surface soil moisture [*Dorigo et al*., 2014] have been assimilated into TERRA_ML within the year 2000 applying an ensemble transform Kalman filter [*Hunt et al*., 2007]. However, no clear improvement has been achieved (not shown). The implementation of the more sophisticated SVAT module VEG3D (CCLM-VEG) clearly reduces the CCLM bias in the Central Sahel (67 mm, 21%), even improving the smaller MPI-ESM bias, but aggravates the result in the Guinea Coast and West Sahel regions. Instead, the application of constant GLC2000 land use maps (CCLM-LUC) reveals a clearly smaller bias in the Guinea Coast region (238 mm, 27%) and a larger one in the West Sahel. More realistic yearly varying land use maps (CCLM-LUV) show hardly any clear impact on the WAM rainfall bias in any region. Altogether, the area-weighted regional mean representing an overall bias assessment for the whole West Africa reveals that all improved boundary and initial conditions are able to slightly reduce the CCLM bias, most obviously the more realistic SSTs (73 mm, 16%). However, none of them can improve the already low MPI-ESM bias.

Thus, the third hypothesis that more realistic boundary conditions and soil initialization are able to reduce WAM rainfall biases of regional predictions can be partly confirmed for some obvious added values of different model improvements over the Guinea Coast (SSTs again strongly, land cover) and Central Sahel (vegetation) but must be rather rejected for the West Sahel. Even if the WAM biases are rather constant across different hindcast decades further simulations need to be performed to verify the stated improvements for CCLM-AOD/SST and CCLM-VEG. The bias reduction strongly depends on the considered boundary or initial condition and region because different model improvements affect various physical processes influencing different West African regions. However, the overall assessment for the whole West Africa reveals slight bias reductions for all model improvements, especially for more realistic SSTs.

In addition, we aim to find possible physical explanations for the three stated added values of different model improvements: The improved Guinea Coast rainfall bias of more realistic ERA-Interim SSTs is linked to reduced SST and ITCZ position biases (not shown) as for coupled regional predictions. Yet the underestimation might be

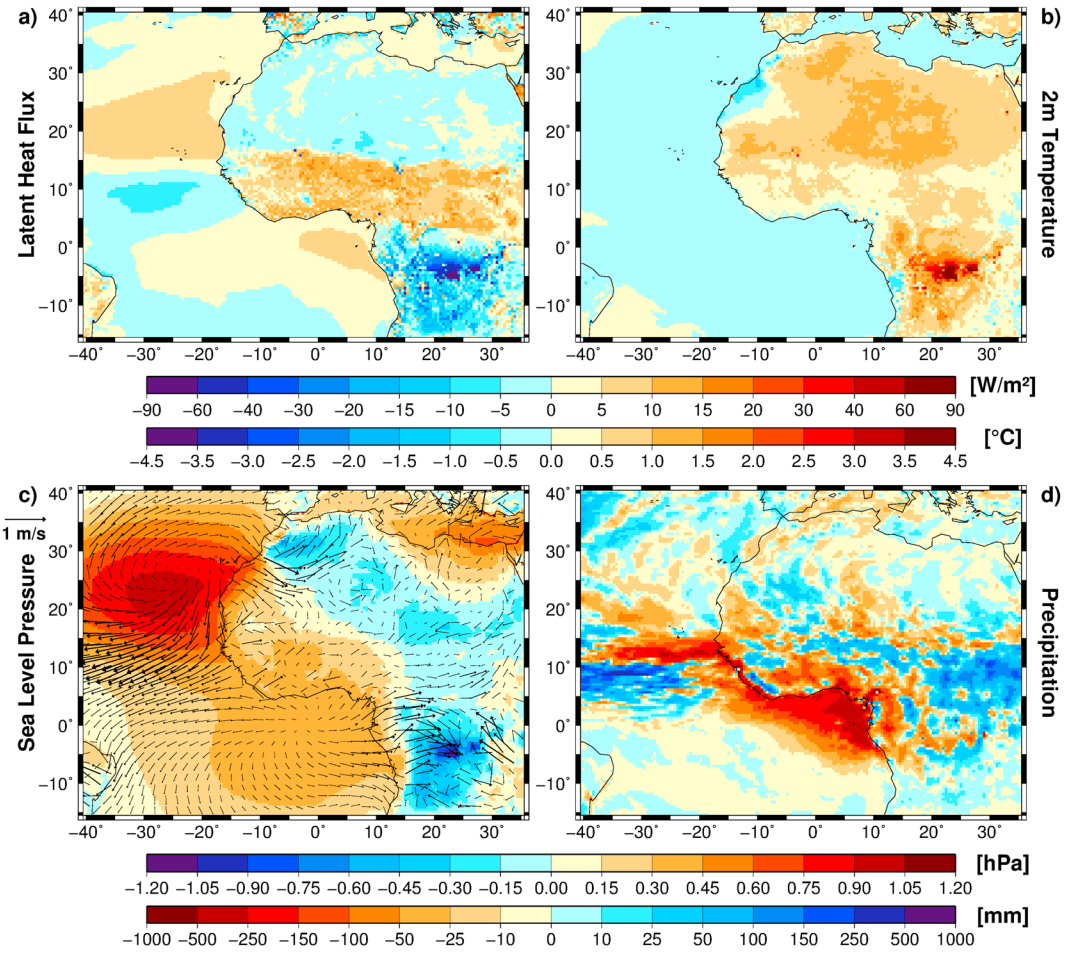

Figure 9. Differences and difference vectors of various simulated atmospheric variables influencing the Guinea Coast rainfall from ensemble means of CCLM-LUC predictions applying improved land cover boundary conditions at 0.44° horizontal resolution averaged over the JJAS season of the 2001–2010 decade compared to CCLM predictions in standard version: (a) latent heat flux, (b) 2 m temperature, (c) sea level pressure (map) with 10 m wind vectors (arrows), and (d) precipitation.

related to deficiencies of reanalysis data, missing atmosphere-ocean feedbacks of uncoupled CCLM, or a generally drier Guinea Coast in CCLM than in REMO due to differing parameterizations. The reduced Central Sahel bias of the improved SVAT module VEG3D can be explained by more realistic higher surface temperatures and a southward shift of the Saharan low-pressure system, the AEJ and AEWs. Thus, associated mesoscale convective systems reveal shorter tracks through the Central Sahel producing less rainfall amounts [*Breil*, 2015].

Possible explanations for the improved Guinea Coast bias of constant GLC2000 land use maps replacing ECOCLIMAP data are found when comparing different atmospheric variables from CCLM-LUC and CCLM during the 2001–2010 decade (Figure 9): Reduced plant cover, evaporation (not shown), and latent heat fluxes over the Congo Basin in CCLM-LUC lead to increased temperatures and lower sea level pressure. Thus, intensified westerlies over the eastern Gulf of Guinea produce rainfall mainly downstream northeast of the Congo Basin. The ascending air masses over the low-pressure area probably intensify the Congo Basin Walker circulation [*Cook and Vizy*, 2015] with compensatory subsidence and increased high pressure over the Gulf of Guinea. Moreover, higher temperatures over the Sahara and increased plant cover, evaporation (not shown), and latent heat fluxes over the Guinea Coast and Sahel intensify West African temperature and moisture gradients and probably also the AEJ [cf. *Cook*, 1999]. The increased mass outflow in the AEJ exit region might generate extended high pressure over the East Atlantic leading to stronger easterlies over the tropical Atlantic. Thus, intensified subsidence with stronger easterlies and westerlies over the Gulf of Guinea diminishes Guinea Coast rainfall. Similar CCLM-LUC results have also been found for other decades (not shown).

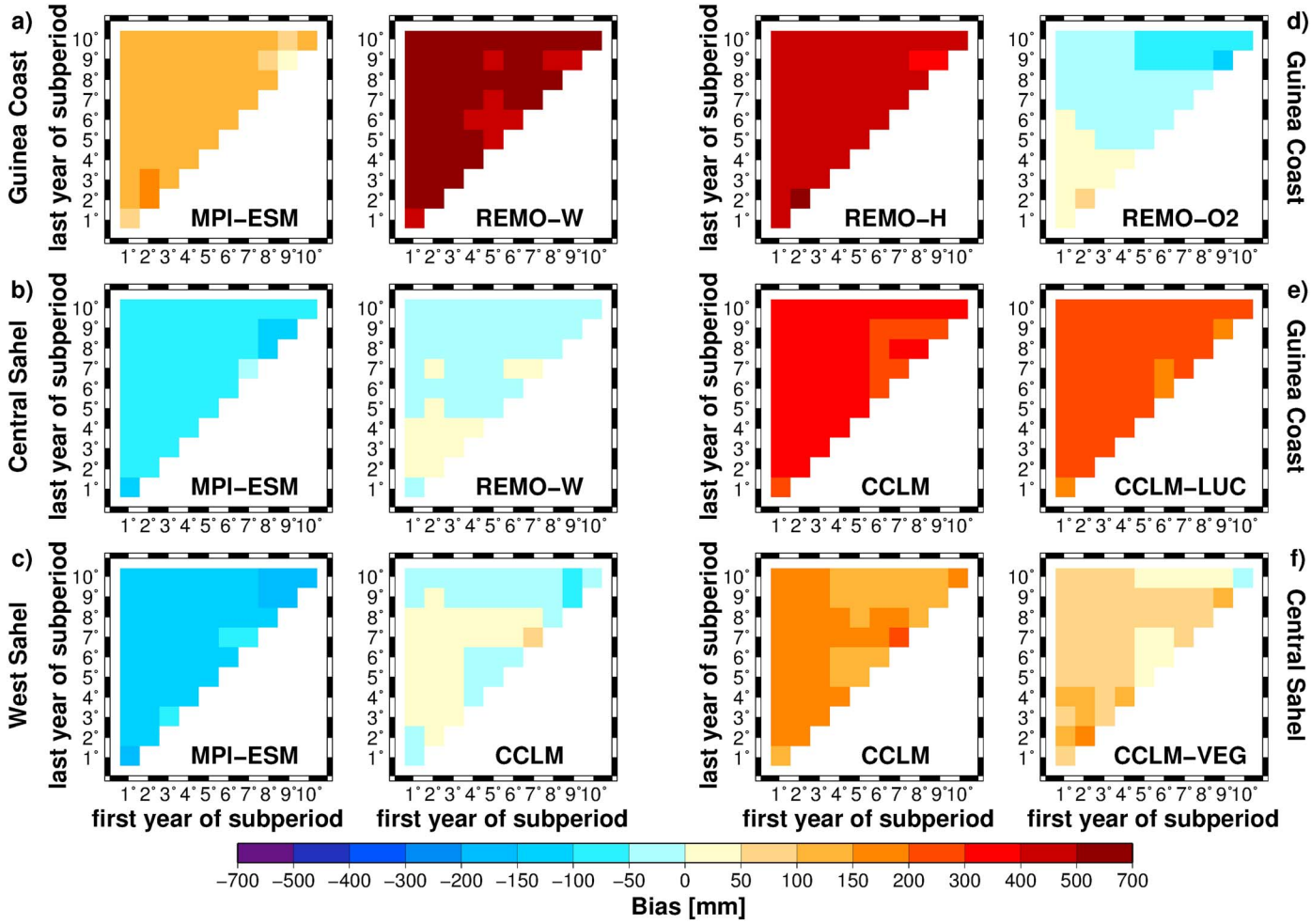

Figure 10. (a–c) Lead-time dependent biases of simulated WAM rainfall from ensemble means of MPI-ESM and (a–f) different regional predictions in standard version, (d) coupled to the MPI-OM ocean model, and (e–f) applying improved land cover and vegetation boundary conditions compared to WMMA observations for selected West African regions and averaged over the JJAS seasons of all available hindcast decades (cf. Table 1). The *x* axis (*y* axis) denotes the first (last) year of all possible subperiods within a decade considered for bias calculation.

Finally, we aim to answer the question if the bias reductions and increases of RCMs and improved boundary and initial conditions presented for decadal means vary for shorter subperiods or different lead times. Figure 10 shows lead-time dependent WAM rainfall biases for all possible subperiods of a decade averaged over all available decades and exemplarily for some prominent bias modifications of this study. MPI-ESM reveals rather small bias variations over different subperiod lengths and lead times in all regions. Largest differences are found for 1 year subperiods over various lead times due to higher variability compared to longer subperiods. RCMs show similar results over the Guinea Coast but slightly larger variations over different lead times even for longer subperiods in the Sahel probably due to larger interannual variability, e.g., of AEWs, on the regional scale. REMO-O2 reveals a small but clear tendency for positive biases at small lead times and larger negative biases at higher lead times over the Guinea Coast possibly related to the long-term memory of the coupled ocean but less variation in the Sahel (not shown). Small variability over different subperiods and lead times is stated for CCLM-LUC over the Guinea Coast. Larger lead-time dependent differences are found for CCLM-VEG, e.g., increased Central Sahel biases for smaller lead times, because only one decade is available revealing higher variability than averages over several decades. For more robust results further decadal simulations need to be performed. Overall, the biases do not clearly increase with higher lead times as probably expected for decadal simulations freely evolving from an initialized starting point. The bias variations over different subperiod lengths and lead times are generally rather small, and stated bias reductions and increases of RCMs and improved boundary and initial conditions are mostly also valid for shorter subperiods and various lead times.

4. Summary and Discussion

This study has analyzed the WAM rainfall biases in decadal climate predictions and addressed the three hypotheses that GCM prediction biases can be improved by dynamical downscaling with (1) a multimodel ensemble of high-resolution RCMs, (2) a RCM coupled to a global ocean model, and (3) a RCM applying more realistic boundary conditions (aerosols, SSTs, vegetation, and land cover) and soil initialization. To test these hypotheses global MPI-ESM predictions have been applied and numerous three-member ensembles of regional predictions with REMO, CCLM, and WRF nested into MPI-ESM have been performed for several hindcast decades.

The global MPI-ESM predictions reveal positive WAM rainfall biases over the Gulf of Guinea and the Guinea Coast and negative ones over the West and Central Sahel resulting in a small negative bias over the whole West Africa. This pattern is induced by an ITCZ southward shift from the northern Guinea Coast (GPCP) to the northern Gulf of Guinea and probably related to a positive SST bias in the tropical East and Southeast Atlantic. These rainfall, ITCZ, and SST biases are common deficiencies of many state-of-the-art coupled GCMs over West Africa [*Martin et al*., 2014; *Richter et al*., 2014] and their relationships have already been described [*Janicot et al*., 1998; *Losada et al*., 2010]. The large SST bias of MPI-ESM seems to be induced by lacking small-scale air-sea interactions due to coarse atmosphere and ocean resolutions causing weaker southerlies along the Namibian coast and even eastward winds and surface ocean currents over the tropical Atlantic [cf. *Grodsky et al*., 2012; *Richter et al*., 2012, 2014].

Concerning the first hypothesis, the impact of dynamical downscaling depends on the considered region and model: Some regional predictions can reduce WAM rainfall biases of MPI-ESM in the West (CCLM, REMO-H) and Central Sahel (REMO-W), but others yield slightly larger biases. Over the tropical Atlantic, Gulf of Guinea, and Guinea Coast all RCMs aggravate the positive GCM bias. The rainfall bias increases or reductions in RCMs cannot be clearly linked to single physical processes but rather to the interactions between various mechanisms: First, similar ITCZ southward shifts to MPI-ESM, smaller for WRF but slightly stronger for all others, are probably related to the Atlantic SST bias inherited from the GCM. Second, differing parameterizations for small-scale convection and turbulent air-sea exchange fluxes might cause stronger westerlies and evaporation over the tropical North Atlantic [cf. *Pu and Cook*, 2010; *Möbis and Stevens*, 2012]. Third, differing land surface conditions probably influence the position and strength of the AEJ and AEWs [cf. *Cook*, 1999]. For the whole West Africa, the already small GCM bias can be further reduced by REMO-H but is enlarged by all other RCMs. The smaller wet biases of REMO-H over the Guinea Coast and West Sahel due to increased minimum cloud heights for rainfall formation show that improved parameterizations can reduce biases [cf. *Klein et al*., 2015]. Overall, the multimodel RCM ensemble mean impairs MPI-ESM over the Guinea Coast and Central Sahel and improves the GCM in the West Sahel but is not able to outperform all individual RCMs in any region. Recent multimodel RCM ensemble studies have found reduced WAM rainfall biases of ensemble means compared to driving global reanalyses but strongly differing biases of single RCMs [*Paeth et al*., 2011; *Nikulin et al*., 2012]. They have stated less positive or even negative biases over the tropical Atlantic, Gulf of Guinea, and Guinea Coast in driving reanalyses and AMIP-type GCMs passed on to the RCMs REMO, CCLM and WRF with partly increased or decreased regional biases [*Druyan et al*., 2010; *Paeth et al*., 2011; *Nikulin et al*., 2012; *Gbobaniyi et al*., 2014].

The second hypothesis that regional predictions coupled to a global ocean model can reduce WAM rainfall biases is clearly confirmed. The Atlantic SST bias is strongly reduced in coupled regional predictions due to fine-scale air-sea interactions at high atmosphere and ocean resolutions [*Sein et al*., 2015]. They improve deficient GCM winds and surface ocean currents, intensify the cold water upwelling of the Benguela current, and reduce the southward expansion of the warm Angola current [cf. *Grodsky et al*., 2012; *Richter et al*., 2012, 2014]. Thus, the simulated ITCZ is not shifted southward but captures the observed position over the northern Guinea Coast. The large WAM rainfall biases of REMO-H and MPI-ESM over the tropical Atlantic, Gulf of Guinea, and Guinea Coast are reduced. Some improvements can also be identified in the Central Sahel but not in the West Sahel. For the whole West Africa, the small MPI-ESM bias can be clearly diminished to almost zero. Coupled regional model studies have found similar added values in simulating regional climate and ocean features, e.g., SST, wind, or rainfall, compared to uncoupled RCMs over different ocean basins [*Ratnam et al*., 2008; *Sein et al*., 2015]. H. Paeth and 14 coauthors (manuscript in preparation, 2015) have analyzed the decadal predictability of the prevailing multimodel RCM ensemble for WAM rainfall and found some enhanced correlations of coupled regional predictions to observations in all regions, mainly the Guinea Coast and West Sahel. However, they have stated an incoherent pattern over all decades despite reduced rainfall and SST biases and improved correlations to observed Atlantic SSTs.

Concerning the third hypothesis, the impacts of more realistic boundary conditions and soil initialization in regional predictions on WAM rainfall biases depend on the considered region and model improvement: Over the Guinea Coast, the statistical bias correction of MPI-ESM SSTs with more realistic reanalyses strongly reduces the WAM rainfall bias due to an improved ITCZ position (similar to coupled regional predictions) but underestimates observations. The constant GLC2000 land use map also shows an improved Guinea Coast bias compared to ECOCLIMAP data because altered land surface conditions probably intensify the AEJ activity and the Congo Basin Walker circulation [*Cook and Vizy*, 2015] shifting Guinea Coast rainfall to the tropical Atlantic and Congo Basin. However, the more realistic yearly varying land use map generated by ASLUCM does not reveal any clear impact on WAM bias in any region but rather some added values in predictability (H. Paeth and 14 coauthors, manuscript in preparation, 2015). In the Central Sahel, the more sophisticated SVAT module VEG3D with explicit vegetation layer reveals some clear bias reduction compared to TERRA_ML, even diminishing the smaller MPI-ESM bias, due to improved soil-vegetation-atmosphere interactions inducing higher surface temperatures and a southward shift of the Saharan heat low, the AEJ, and AEWs [*Breil*, 2015]. In the West Sahel, the almost zero bias of CCLM can be reached by a combination of AeroCom AODs and ERA-Interim SSTs but not further reduced by any model improvement. The higher-resolved AOD climatology from AeroCom [*Kinne et al*., 2006] does not considerably reduce the WAM rainfall bias in any region compared with that from *Tanré et al*. [1984] which overrates AODs over North Africa and underrates summer AODs over Central Africa [*Kothe et al*., 2014b]. Both methods of optimizing soil initialization with a TERRA_ML spin-up run, i.e., forcing with realistic atmospheric data and assimilation of satellite-based soil moistures, cannot clearly improve the bias of the already well performing reanalysis driven soil spin-up run in any region. They rather reveal some enhancements in predictability (H. Paeth and 14 coauthors, manuscript in preparation, 2015). For the whole West Africa, the CCLM bias is slightly reduced by all improved boundary and initial conditions, mainly by more realistic SSTs. Even if the WAM biases are rather constant across various decades, subperiods of decades and lead times further decadal simulations are still needed to robustly confirm the stated bias reductions due to different model improvements. These results partly confirm partly controvert the clear improvements of simulated WAM rainfall bias (and predictability) due to more realistic atmospheric, oceanic, or terrestrial initial or boundary conditions found in several research studies [e.g., *Paeth and Hense*, 2004; *Xue et al*., 2004; *Paeth and Feichter*, 2006; *Douville et al*., 2007; *Abiodun et al*., 2008]. In addition, improved aerosol and vegetation boundary conditions can reduce temperature biases over West Africa (not shown).

5. Conclusions

In summary, the hypotheses of this study are evaluated separately per region: Over the Guinea Coast, the WAM rainfall bias of global predictions is aggravated by dynamical downscaling, but model improvements (ocean coupling, more realistic SSTs, or land cover) lead to bias reduction. In the Sahel, the GCM bias is improved by regional predictions with different RCMs for each region and further reduced by ocean coupling and improved vegetation in the Central Sahel. For West Africa, regional predictions with REMO-H and ocean coupling diminish the small MPI-ESM bias to nearly zero. Yet even if the biases are consistent across decades, some stated results still need to be confirmed by further simulations.

From these findings two major conclusions can be drawn: First, the regional predictions coupled to a global ocean model successfully reduce the tropical Atlantic SST bias inherited from global predictions, reflecting a prominent problem of many state-of-the-art GCMs [*Richter et al*., 2014], and improve both ITCZ position and WAM rainfall biases. This result is promising for decadal climate impact research on food and water security or hazard management in West Africa. Second, the impacts of RCMs, ocean coupling, and improved boundary or initial conditions strongly depend on the considered region because various model parameterizations or improvements affect different physical processes influencing various regions. Dynamical downscaling or model improvements do not contribute to bias reduction in every region, but only where high resolution or additional complexity improve the related physical processes instead of adding useless noise. Model parameterizations or improvements calibrated for a certain region might even cause aggravation in another region. In this study, some rather robust factors for bias reduction of WAM rainfall have been identified which might enable to set up the optimal combination of influencing factors yielding the smallest bias for a certain region. Assuming stationarity of biases this selection might be transferred to decadal predictions for the near future, and the corresponding interdecadal variation of biases might serve as a measure of uncertainty for future predictions. However, further sensitivity studies need to be performed to be able to support policy

makers in selecting the best model combination for climate impact research in a particular West African region. Our study is a first step into this direction.

Some aspects of this study are still subject to uncertainties or motivate further research: A major uncertainty is the relatively small sample size of ensemble members and hindcast decades which could not be increased due to limited computer resources and numerous model versions. However, the WAM rainfall biases are rather consistent over different decades (see Figures 1 and 8) and ensemble members (not shown). Another uncertainty is the use of only one global prediction system. Even if the Atlantic SST bias is a common problem of many GCMs [*Richter et al.*, 2014] a multimodel approach might also be interesting for global predictions to consider the spread of rainfall biases due to various model configurations, parameterizations, or resolutions [*Martin et al.*, 2014]. To compare the impacts of ocean coupling and improved boundary conditions in different RCMs further sensitivity studies are planned for CCLM with coupled ocean and for REMO and WRF with more realistic AOD climatology and constant as well as yearly varying land cover maps. We are also preparing RCM experiments with yearly changing AOD boundary conditions. Further investigations are currently dedicated to surface temperature and rainfall extremes in West Africa and Atlantic tropical cyclones probably revealing similar improvements due to dynamical downscaling, ocean coupling, and more realistic boundary and initial conditions.

Acknowledgments

This study has been carried out in the framework of the German MiKlip project and supported by the German Minister of Education and Research (BMBF) under grant 01LP1129A–F. Furthermore, Dmitry Sein has been supported by the BMBF under the research grant 03G0835B of the project SPACES-AGULHAS. We thank Kevin Sieck for assistance with the setup of REMO simulations and Robert Redl for supporting the AEJ and AEW analysis. We acknowledge the Max-Planck Institute for Meteorology, the ECMWF, the IIASA, the Joint Research Centre, the FAO, OpenStreetMap, the University of Delaware, the NASA-GSFC, the Climatic Research Unit, and the ESA for providing the MPI-ESM decadal predictions, the ERA40, ERA-Interim and ORAS4 reanalyses, the WATCH-WFDEI data set, the GLC2000 land use data set, the FAO statistical data sets, the street data set, the Willmott-Matsuura data set, the GPCP data sets, the CRU data set, and the ESA CCI soil moisture data set, respectively. All data applied in this study can be obtained from the stated references. The RCM predictions have been performed by the authors of this study and can be made available on request.

References

Abiodun, B. J., J. S. Pal, E. A. Afiesimama, W. J. Gutowski, and A. Adedoyin (2008), Simulation of West African monsoon using RegCM3 Part II: Impacts of deforestation and desertification, *Theor. Appl. Climatol.*, *93*(3–4), 245–261, doi:10.1007/s00704-007-0333-1.

Adler, R. F., et al. (2003), The version 2 global precipitation climatology project (GPCP) monthly precipitation analysis (1979–present), *J. Hydrometeorol.*, *4*(6), 1147–1167, doi:10.1175/1525-7541(2003)004<1147:TVGPCP>2.0.CO;2.

Alo, C. A., and G. Wang (2010), Role of vegetation dynamics in regional climate predictions over western Africa, *Clim. Dyn.*, *35*(5), 907–922, doi:10.1007/s00382-010-0744-z.

Balmaseda, M. A., K. Mogensen, and A. T. Weaver (2013), Evaluation of the ECMWF ocean reanalysis system ORAS4, *Q. J. R. Meteorol. Soc.*, *139*(674), 1132–1161, doi:10.1002/qj.2063.

Balsamo, G., et al. (2015), ERA-Interim/Land: A global land surface reanalysis data set, *Hydrol. Earth Syst. Sci.*, *19*(1), 389–407, doi:10.5194/hess-19-389-2015.

Bartholomé, E., and A. S. Belward (2005), GLC2000: A new approach to global land cover mapping from Earth observation data, *Int. J. Remote Sens.*, *26*(9), 1959–1977, doi:10.1080/01431160412331291297.

Bellucci, A., et al. (2015), Advancements in decadal climate predictability: The role of nonoceanic drivers, *Rev. Geophys.*, *53*, 165–202, doi:10.1002/2014RG000473.

Benson, C., and E. J. Clay (1998), The impact of drought on sub-Saharan economies, World Bank Tech. Paper No. 401, Overseas Development Institute, Regent's College, London, U. K., doi:10.1596/0-8213-4180-4.

Berry, G. J., C. D. Thorncroft, and T. Hewson (2007), African easterly waves during 2004—Analysis using objective techniques, *Mon. Weather Rev.*, *135*(4), 1251–1267, doi:10.1175/MWR3343.1.

Braun, F. J., and G. Schädler (2005), Comparison of soil hydraulic parameterizations for mesoscale meteorological models, *J. Appl. Meteorol.*, *44*(7), 1116–1132, doi:10.1175/JAM2259.1.

Breil, M. (2015), Einfluss der Boden-Vegetation-Atmosphären Wechselwirkungen auf die dekadische Vorhersagbarkeit des Westafrikanischen Monsuns, PhD thesis, Department of Civil Engineering, Geo and Environmental Sciences – Karlsruhe Institute of Technology (KIT), Univ. of Karlsruhe, Karlsruhe, Germany.

Champeaux, J. L., V. Masson, and F. Chauvin (2005), ECOCLIMAP: A global database of land surface parameters at 1 km resolution, *Meteorol. Appl.*, *12*(1), 29–32, doi:10.1017/S1350482705001519.

Chatelain, C., L. Gautier, and R. Spichiger (1996), A recent history of forest fragmentation in southwestern Ivory Coast, *Biodiversity Conserv.*, *5*(1), 37–53, doi:10.1007/BF00056291.

Cook, K. H. (1999), Generation of the African easterly jet and its role in determining West African precipitation, *J. Clim.*, *12*(5), 1165–1184, doi:10.1175/1520-0442(1999)012<1165:GOTAEJ>2.0.CO;2.

Cook, K. H., and E. K. Vizy (2015), The Congo Basin Walker circulation: Dynamics and connections to precipitation, *Clim. Dyn.*, 1–21, doi:10.1007/s00382-015-2864-y.

Dee, D. P., et al. (2011), The ERA-Interim reanalysis: Configuration and performance of the data assimilation system, *Q. J. R. Meteorol. Soc.*, *137*(656), 553–597, doi:10.1002/qj.828.

Diatta, S., and A. H. Fink (2014), Statistical relationship between remote climate indices and West African monsoon variability, *Int. J. Climatol.*, *34*(12), 3348–3367, doi:10.1002/joc.3912.

Dorigo, W. A., et al. (2014), Evaluation of the ESA CCI soil moisture product using ground-based observations, *Remote Sens. Environ.*, *162*, 380–395, doi:10.1016/j.rse.2014.07.023.

Douville, H., S. Conil, S. Tyteca, and A. Voldoire (2007), Soil moisture memory and West African monsoon predictability: Artifact or reality, *Clim. Dyn.*, *28*(7–8), 723–742, doi:10.1007/s00382-006-0207-8.

Druyan, L. M., et al. (2010), The WAMME regional model intercomparison study, *Clim. Dyn.*, *35*(1), 175–192, doi:10.1007/s00382-009-0676-7.

Dunstone, N. J., D. M. Smith, and R. Eade (2011), Multi-year predictability of the tropical Atlantic atmosphere driven by the high latitude North Atlantic Ocean, *Geophys. Res. Lett.*, *38* L14701, doi:10.1029/2011GL047949.

Fink, A. H., and A. Reiner (2003), Spatiotemporal variability of the relation between African easterly waves and West African squall lines in 1998 and 1999, *J. Geophys. Res.*, *108*(D11), 4332, doi:10.1029/2002JD002816.

Fink, A. H., H. Paeth, V. Ermert, S. Pohle, and M. Diederich (2010), Meteorological processes influencing the weather and climate of Benin (Chapter I-5.1), in *Impacts of Global Change on the Hydrological Cycle in West and Northwest Africa*, edited by P. Speth et al., pp. 135–149, Springer, Berlin, Germany, doi:10.1007/978-3-642-12957-5.

Flaounas, E., S. Bastin, and S. Janicot (2011), Regional climate modelling of the 2006 West African monsoon: Sensitivity to convection and planetary boundary layer parameterisation using WRF, *Clim. Dyn.*, *36*(5–6), 1083–1105, doi:10.1007/s00382-010-0785-3.
Gaetani, M., and E. Mohino (2013), Decadal prediction of the Sahel precipitation in CMIP5 simulations, *J. Clim.*, *26*(19), 7708–7719, doi:10.1175/JCLI-D-12-00635.1.
Gbobaniyi, E., et al. (2014), Climatology, annual cycle and interannual variability of precipitation and temperature in CORDEX simulations over West Africa, *Int. J. Climatol.*, *34*(7), 2241–2257, doi:10.1002/joc.3834.
Grodsky, S. A., J. A. Carton, S. Nigam, and Y. M. Okumura (2012), Tropical Atlantic biases in CCSM4, *J. Clim.*, *25*(11), 3684–3701, doi:10.1175/JCLI-D-11-00315.1.
Hawkins, E., B. Dong, J. Robson, and R. Sutton (2014), The interpretation and use of biases in decadal climate predictions, *J. Clim.*, *27*(8), 2931–2947, doi:10.1175/JCLI-D-13-00473.1.
Hazeleger, W., V. Guemas, B. Wouters, S. Corti, I. Andreu-Burillo, F. J. Doblas-Reyes, K. Wyser, and M. Caian (2013), Multiyear climate predictions using two initialization strategies, *Geophys. Res. Lett.*, *40*, 1794–1798, doi:10.1002/grl.50355.
Hu, Z.-Z., B. Huang, Y.-T. Hou, W. Wang, F. Yang, C. Stan, and E. K. Schneider (2010), Sensitivity of tropical climate to low-level clouds in the NCEP climate forecast system, *Clim. Dyn.*, *36*(9–10), 1795–1811, doi:10.1007/s00382-010-0797-z.
Huffman, G. J., R. F. Adler, M. Morrissey, D. T. Bolvin, S. Curtis, R. Joyce, B. McGavock, and J. Susskind (2001), Global precipitation at one-degree daily resolution from multi-satellite observations, *J. Hydrometeorol.*, *2*(1), 36–50, doi:10.1175/1525-7541(2001)002<0036:GPAODD>2.0.CO;2.
Huffman, G. J., R. F. Adler, D. T. Bolvin, and G. Gu (2009), Improving the global precipitation record: GPCP version 2.1, *Geophys. Res. Lett.*, *36*, L17808, doi:10.1029/2009GL040000.
Hunt, B. R., E. Kostelich, and I. Szunyogh (2007), Efficient data assimilation for spatiotemporal chaos: A local ensemble transform Kalman filter, *Phys. D*, *230*(1–2), 112–126, doi:10.1016/j.physd.2006.11.008.
Jacob, D. (2001), A note to the simulation of the annual and interannual variability of the water budget over the Baltic Sea drainage basin, *Meteorol. Atmos. Phys.*, *77*(1–4), 61–74, doi:10.1007/s007030170017.
Jacob, D., et al. (2007), An inter-comparison of regional climate models for Europe: Model performance in present-day climate, *Clim. Change*, *81*(1 Supplement), 31–52, doi:10.1007/s10584-006-9213-4.
Janicot, S., A. Harzallah, B. Fontaine, and V. Moron (1998), West African monsoon dynamics and eastern equatorial Atlantic and Pacific SST anomalies (1970–88), *J. Clim.*, *11*(8), 1874–1882.
Jungclaus, J. H., N. Fischer, H. Haak, K. Lohmann, J. Marotzke, D. Matei, U. Mikolajewicz, D. Notz, and J. S. von Storch (2013), Characteristics of the ocean simulations in MPIOM, the ocean component of the MPI-Earth system model, *J. Adv. Model. Earth Syst.*, *5*(2), 422–446, doi:10.1002/jame.20023.
Keenlyside, N. S., M. Latif, J. Jungclaus, L. Kornblueh, and E. Roeckner (2008), Advancing decadal-scale climate prediction in the North Atlantic sector, *Nature*, *453*(7191), 84–88, doi:10.1038/nature06921.
Kharin, V. V., G. J. Boer, W. J. Merryfield, J. F. Scinocca, and W.-S. Lee (2012), Statistical adjustment of decadal predictions in a changing climate, *Geophys. Res. Lett.*, *39*, L19705, doi:10.1029/2012GL052647.
Kim, H.-M., P. J. Webster, and J. A. Curry (2012), Evaluation of short-term climate change prediction in multi-model CMIP5 decadal hindcasts, *Geophys. Res. Lett.*, *39*, L10701, doi:10.1029/2012GL051644.
Kinne, S., et al. (2006), An AeroCom initial assessment: Optical properties in aerosol component modules of global models, *Atmos. Chem. Phys.*, *6*(7), 1815–1834, doi:10.5194/acp-6-1815-2006.
Klein, C., D. Heinzeller, J. Bliefernicht, and H. Kunstmann (2015), Variability of West African monsoon patterns generated by a WRF multi-physics ensemble, *Clim. Dyn.*, *45*, 2733–2755, doi:10.1007/s00382-015-2505-5.
Kothe, S., D. Lüthi, and B. Ahrens (2014a), Analysis of the West African Monsoon system in the regional climate model COSMO-CLM, *Int. J. Climatol.*, *34*(2), 481–493, doi:10.1002/joc.3702.
Kothe, S., H.-J. Panitz, and B. Ahrens (2014b), Analysis of the radiation budget in regional climate simulations with COSMO-CLM for Africa, *Meteorolog. Z.*, *23*(2), 123–141, doi:10.1127/0941-2948/2014/0527.
Losada, T., B. Rodríguez-Fonseca, S. Janicot, S. Gervois, F. Chauvin, and P. Ruti (2010), A multi-model approach to the Atlantic Equatorial mode: Impact on the West African monsoon, *Clim. Dyn.*, *35*(1), 29–43, doi:10.1007/s00382-009-0625-5.
Losada, T., B. Rodriguez-Fonseca, E. Mohino, J. Bader, S. Janicot, and C. R. Mechoso (2012), Tropical SST and Sahel rainfall: A non-stationary relationship, *Geophys. Res. Lett.*, *39*, L12705, doi:10.1029/2012GL052423.
Martin, E. R., and C. Thorncroft (2014), Sahel rainfall in multimodel CMIP5 decadal hindcasts, *Geophys. Res. Lett.*, *41*, 2169–2175, doi:10.1002/2014GL059338.
Martin, E. R., C. Thorncroft, and B. B. B. Booth (2014), The multidecadal Atlantic SST—Sahel rainfall teleconnection in CMIP5 simulations, *J. Clim.*, *27*(2), 784–806, doi:10.1175/JCLI-D-13-00242.1.
Matei, D., H. Pohlmann, J. Jungclaus, W. Müller, H. Haak, and J. Marotzke (2012), Two tales of initializing decadal climate prediction experiments with the ECHAM5/MPI-OM model, *J. Clim.*, *25*(24), 8502–8523, doi:10.1175/JCLI-D-11-00633.1.
Meehl, G. A., et al. (2009), Decadal prediction – Can it be skilful?, *Bull. Am. Meteorol. Soc.*, *90*(10), 1467–1485, doi:10.1175/2009BAMS2778.1.
Mehta, V. M., H. Wang, and K. Mendoza (2013), Decadal predictability of tropical ocean basin average and global average sea surface temperatures in CMIP5 experiments with the HadCM3, GFDL-CM2.1, NCAR-CCSM4, and MIROC5 global Earth system models, *Geophys. Res. Lett.*, *40*, 2807–2812, doi:10.1002/grl.50236.
Mitchell, T. D., and P. D. Jones (2005), An improved method of constructing a database of monthly climate observations and associated high-resolution grids, *Int. J. Climatol.*, *25*(6), 693–712, doi:10.1002/joc.1181.
Miyasaka, T., and H. Nakamura (2005), Structure and formation mechanisms of the Northern Hemisphere summertime subtropical highs, *J. Clim.*, *18*(23), 5046–5065, doi:10.1175/JCLI3599.1.
Möbis, B., and B. Stevens (2012), Factors controlling the position of the Intertropical Convergence Zone on an aquaplanet, *J. Adv. Model. Earth Syst.*, *4*, M00A04, doi:10.1029/2012MS000199.
Moss, R. H., et al. (2010), The next generation of scenarios for climate change research and assessment, *Nature*, *463*(7282), 747–756, doi:10.1038/nature08823.
Moufouma-Okia, W., and D. P. Rowell (2010), Impact of soil moisture initialisation and lateral boundary conditions on regional climate model simulations of the West African monsoon, *Clim. Dyn.*, *35*(10), 213–229, doi:10.1007/s00382-009-0638-0.
Murphy, J., V. Kattsov, N. Keenlyside, M. Kimoto, G. Meehl, V. Mehta, H. Pohlmann, A. Scaife, and D. Smith (2010), Towards prediction of decadal climate variability and change, *Proc. Environ. Sci.*, *1*, 287–304, doi:10.1016/j.proenv.2010.09.018.
Nicholson, S. E., and I. M. Palao (1993), A re-evaluation of rainfall variability in the Sahel. Part 1. Characteristics of rainfall fluctuations, *Int. J. Climatol.*, *13*(4), 371–389, doi:10.1002/joc.v13:4.
Nikulin, G., et al. (2012), Precipitation climatology in an ensemble of CORDEX-Africa regional climate simulations, *J. Clim.*, *25*(18), 6057–6078, doi:10.1175/JCLI-D-11-00375.1.

Paeth, H., and A. Hense (2004), SST versus climate change signals in West African rainfall: 20th century variations and future projections, *Clim. Change*, *65*(1–2), 179–208, doi:10.1023/B:CLIM.0000037508.88115.8a.
Paeth, H., and J. Feichter (2006), Greenhouse-gas versus aerosol forcing and African climate response, *Clim. Dyn.*, *26*(1), 35–54, doi:10.1007/s00382-005-0070-z.
Paeth, H., K. Born, R. Podzun, and D. Jacob (2005), Regional dynamical downscaling over West Africa: Model evaluation and comparison of wet and dry years, *Meteorol. Z.*, *14*(3), 349–367, doi:10.1127/0941-2948/2005/0038.
Paeth, H., K. Born, R. Girmes, R. Podzun, and D. Jacob (2009), Regional climate change in tropical Africa under greenhouse forcing and land-use changes, *J. Clim.*, *22*(1), 114–132, doi:10.1175/2008JCLI2390.1.
Paeth, H., et al. (2011), Progress in regional downscaling of West African precipitation, *Atmos. Sci. Lett.*, *12*(1), 75–82, doi:10.1002/asl.306.
Panitz, H.-J., A. Dosio, M. Büchner, D. Lüthi, and K. Keuler (2014), COSMO-CLM (CCLM) climate simulations over CORDEX Africa domain: analysis of the ERA-interim driven simulations at 0.44° and 0.22° resolution, *Clim. Dyn.*, *42*(11–12), 3015–3038, doi:10.1007/s00382-013-1834-5.
Paxian, A., E. Hertig, G. Vogt, S. Seubert, J. Jacobeit, and H. Paeth (2014), Greenhouse gas related predictability of regional climate model trends in the Mediterranean area, *Int. J. Climatol.*, *34*(7), 2293–2307, doi:10.1002/joc.3838.
Paxian, A., E. Hertig, S. Seubert, G. Vogt, J. Jacobeit, and H. Paeth (2015), Present-day and future Mediterranean precipitation extremes assessed by different statistical approaches, *Clim. Dyn.*, *44*(3–4), 845–860, doi:10.1007/s00382-014-2428-6.
Pohlmann, H., W. A. Müller, K. Kulkarni, M. Kameswarrao, D. Matei, F. S. E. Vamborg, C. Kadow, S. Illing, and J. Marotzke (2013), Improved forecast skill in the tropics in the new MiKlip decadal climate predictions, *Geophys. Res. Lett.*, *40*, 5798–5802, doi:10.1002/2013GL058051.
Pu, B., and K. H. Cook (2010), Dynamics of the West African westerly jet, *J. Clim.*, *23*(23), 6263–6276, doi:10.1175/2010JCLI3648.1.
Ramage, C. S. (1995), *Forecasters Guide to Tropical Meteorology—AWS TR 240 Updated, AWS/TR-95/001*, Air Weather Service, Scott Air Force Base, Ill.
Ratnam, J. V., F. Giorgi, A. Kaginalkar, and S. Cozzini (2008), Simulation of the Indian monsoon using the RegCM3-ROMS regional coupled model, *Clim. Dyn.*, *33*(1), 119–139, doi:10.1007/s00382-008-0433-3.
Reifen, C., and R. Toumi (2009), Climate projections: Past performance no guarantee of future skill?, *Geophys. Res. Lett.*, *36*, L13704, doi:10.1029/2009GL038082.
Richter, I., S.-P. Xie, A. T. Wittenberg, and Y. Masumoto (2012), Tropical Atlantic biases and their relation to surface wind stress and terrestrial precipitation, *Clim. Dyn.*, *38*, 985–1001, doi:10.1007/s00382-011-1038-9.
Richter, I., S. P. Xie, S. Behera, T. Doi, and Y. Masumoto (2014), Equatorial Atlantic variability and its relation to mean state biases in CMIP5, *Clim. Dyn.*, *42*(1–2), 171–188, doi:10.1007/s00382-012-1624-5.
Rockel, B., A. Will, and A. Hense (2008), The regional climate model COSMO-CLM (CCLM), *Meteorol. Z.*, *17*(4), 347–348, doi:10.1127/0941-2948/2008/0309.
Rodriguez-Fonseca, B., et al. (2011), Interannual and decadal SST-forced responses of the West African monsoon, *Atmos. Sci. Lett.*, *12*(1), 67–74, doi:10.1002/asl.308.
Rowell, D. P. (2013), Simulating SST teleconnections to Africa: What is the state of the art?, *J. Clim.*, *26*(15), 5397–5418, doi:10.1175/JCLI-D-12-00761.1.
Schrodin, R., and E. Heise (2002), A new multi-layer soil-model, in *COSMO Newsletter No. 2 February 2002*, pp. 149–151, Deutscher Wetterdienst, Offenbach, Germany.
Sein, D. V., N. Koldunov, J. Pinto, and W. Cabos (2014), Sensitivity of simulated regional Arctic climate to the choice of coupled model domain, *Tellus A*, *66*, 23,966, doi:10.3402/tellusa.v66.23966.
Sein, D. V., U. Mikolajewicz, M. Gröger, I. Fast, W. Cabos, J. G. Pinto, S. Hagemann, T. Semmler, A. Izquierdo, and D. Jacob (2015), Regionally coupled atmosphere-ocean-sea ice marine biogeochemistry model ROM: 1. Description and validation, *J. Adv. Model. Earth Syst.*, *7*, 268–304, doi:10.1002/2014MS000357.
Siongco, A. C., C. Hohenegger, and B. Stevens (2015), The Atlantic ITCZ bias in CMIP5 models, *Clim. Dyn.*, *45*(5), 1169–1180, doi:10.1007/s00382-014-2366-3.
Skamarock, W. C., J. B. Klemp, J. Dudhia, D. O. Gill, D. M. Barker, M. G. Duda, X.-Y. Huang, W. Wang, and J. G. Powers (2008), A description of the advanced research WRF version 3, NCAR Tech. Note 475, NCAR, Boulder, Colo.
Smith, D., et al. (2013), Real-time multi-model decadal climate predictions, *Clim. Dyn.*, *41*(11–12), 2875–2888, doi:10.1007/s00382-012-1600-0.
Solmon, F., N. Elguindi, and M. Mallet (2012), Radiative and climatic effects of dust over West Africa, as simulated by a regional climate model, *Clim. Res.*, *52*, 97–113, doi:10.3354/cr01039.
Stevens, B., et al. (2013), Atmospheric component of the MPI-M Earth system model: ECHAM6, *J. Adv. Model. Earth Syst.*, *5*, 146–172, doi:10.1002/jame.20015.
Sylla, M. B., E. Coppola, L. Mariotti, F. Giorgi, P. M. Ruti, A. Dell'Aquila, and X. Bi (2010), Multiyear simulation of the African climate using a regional climate model (RegCM3) with the high resolution ERA-interim reanalysis, *Clim. Dyn.*, *35*(1), 231–247, doi:10.1007/s00382-009-0613-9.
Tanré, D., J. Geleyn, and J. Slingo (1984), First results of the introduction of an advanced aerosol-radiation interaction in ECMWF low resolution global model. Aerosols and Their Climatic Effects, in *Aerosols and Their Climatic Effects*, edited by H. Gerber and A. Deepak, pp. 133–177, A. Deepak Pub, Hampton, Va.
Tozuka, T., T. Doi, T. Miyasaka, N. Keenlyside, and T. Yamagata (2011), Key factors in simulating the equatorial Atlantic zonal sea surface temperature gradient in a coupled general circulation model, *J. Geophys. Res.*, *116*, C06010, doi:10.1029/2010JC006717.
Uppala, S., et al. (2005), The ERA-40 re-analysis, *Q. J. R. Meteorol. Soc.*, *131*(612), 2961–3012, doi:10.1256/qj.04.176.
van Oldenborgh, G. J., F. J. Doblas-Reyes, B. Wouters, and W. Hazeleger (2012), Decadal prediction skill in a multi-model ensemble, *Clim. Dyn.*, *38*(7–8), 1263–1280, doi:10.1007/s00382-012-1313-4.
Weedon, G. P., G. Balsamo, N. Bellouin, S. Gomes, M. J. Best, and P. Viterbo (2014), The WFDEI meteorological forcing data set: WATCH Forcing Data methodology applied to ERA-Interim reanalysis data, *Water Resour. Res.*, *50*, 7505–7514, doi:10.1002/2014WR015638.
Xue, Y., H. M. H. Juang, W. Li, S. Prince, R. DeFries, Y. Jiao, and R. Vasic (2004), Role of land surface processes in monsoon development: East Asia and West Africa, *J. Geophys. Res.*, *109*, D03105, doi:10.1029/2003JD003556.